

**TEST VERSUS PREDICTIONS FOR ROTORDYNAMIC AND LEAKAGE
CHARACTERISTICS OF A CONVERGENT-TAPERED, HONEYCOMB-
STATOR/SMOOTH-ROTOR ANNULAR GAS SEAL**

A Thesis

by

DANIEL EDUARDO VAN DER VELDE ALVAREZ

Submitted to the Office of Graduate Studies of
Texas A&M University
in partial fulfillment of the requirements for the degree of

MASTER OF SCIENCE

December 2006

Major Subject: Mechanical Engineering

**TEST VERSUS PREDICTIONS FOR ROTORDYNAMIC AND LEAKAGE
CHARACTERISTICS OF A CONVERGENT-TAPERED, HONEYCOMB-
STATOR/SMOOTH-ROTOR ANNULAR GAS SEAL**

A Thesis

by

DANIEL EDUARDO VAN DER VELDE ALVAREZ

Submitted to the Office of Graduate Studies of
Texas A&M University
in partial fulfillment of the requirements for the degree of

MASTER OF SCIENCE

Approved by:

Chair of Committee, Dara Childs
Committee Members, John Vance
Paul Cizmas
Head of Department, Dennis L. O'Neal

December 2006

Major Subject: Mechanical Engineering

ABSTRACT

Test versus Predictions for Rotordynamic and Leakage Characteristics of a Convergent-Tapered, Honeycomb-Stator/Smooth-Rotor Annular Gas Seal.

(December 2006)

Daniel Eduardo van der Velde Alvarez, B.S., Universidad Simón Bolívar

Chair of Advisory Committee: Dr. Dara W. Childs

This thesis presents the results for measured and predicted rotordynamic coefficients and leakage for a convergent-tapered honeycomb seal (CTHC). The test seals had a diameter of 114.968 mm (4.5263 in) at the entrance, and a diameter of 114.709 mm (4.5161 in) at the exit. The honeycomb cell depth was 3.175 mm (0.125 in), and the cell width was 0.79 mm (0.0311 in). Measurements are reported with air as the test fluid at three different speeds: 10,200, 15,200, and 20,200 rpm; with a supply pressure of 69 bar (1,000 psi), with exit-to-inlet pressure ratios from 20% to 50%, and using two rotors that are 114.3 mm (4.500 in) and 114.5 mm (4.508 in) respectively; this enables the same seals to be tested under two different conditions.

The q factor, which is just a simple way to quantify taper is defined as the taper-angle seal parameter and is calculated using the inlet and exit radial clearance. Two taper-angles parameters were calculated; $q = 0.24$ for the 114.3 mm (4.500 in) rotor, and $q = 0.386$ for the 114.5 mm (4.508 in) rotor. The $q = 0.24$ condition was compared to a constant clearance honeycomb seal (CCHC $q = 0$) because both sets of data were taken with the same rotor diameter.

The direct stiffness, effective stiffness, and direct damping coefficients were larger for $q = 0.24$. The CTHC $q = 0.24$ eliminates the direct negative static stiffness obtained with CCHC ($q = 0$). The cross-coupled stiffness and damping also were larger for $q = 0.24$, especially at low frequencies.

Effective damping is one of the best indicators in determining the stability of a roughened stator annular gas seal. The frequency at which it changes sign is called the

cross-over frequency. In applications, this frequency needs to be lower than the rotor-system's first natural frequency. Otherwise, the seal will be highly destabilizing instead of highly stabilizing. The magnitude of effective damping and the cross-over frequency also increases with q for all frequencies.

Constant clearance honeycomb seals have less leakage than convergent-tapered honeycomb seals. CTHC ($q = 0.24$), has approximately 20 percent more leakage than CCHC ($q = 0$).

The experimental results for rotordynamic characteristics and leakage were compared to theoretical predictions by the two-control-volume developed by Kleynhans and Childs. All rotordynamic coefficients were reasonably predicted for all cases. The model does a better job predicting the cross-coupled stiffness and damping coefficients rather than the direct stiffness and damping coefficients. Also, the two-control-volume model predicts the dynamic characteristics of CCHC ($q = 0$) better, and does not predict well the effective stiffness and damping for CTHC $q = 0.386$.

ACKNOWLEDGEMENTS

I would like to thank Dr. Dara W. Childs for allowing me such an excellent opportunity to learn working with him at the turbomachinery laboratory. It was a marvelous and unforgettable experience.

I would like to thank Elizabeth Veenstra for all her help with the seal testing. I would also like to thank Stephen Phillips, Eddie Denk and Clint Carter for all their help during our many trouble-shooting sessions. I could not have completed my testing without their help.

I would like to thank my parents, Luis Eduardo and Maria Concepción van der Velde, and my brother, Luis E. van der Velde. They have always supported me in everything that I do.

Finally, I need to thank my wife, Margarita Rodrigues, for her help, support, and enthusiasm in all that I do in my life, but especially my master's degree because she went through the same experience with me all the time, and we both finished it successfully. I never would have accomplished this if not for her.

TABLE OF CONTENTS

	Page
ABSTRACT	iii
ACKNOWLEDGEMENTS	v
TABLE OF CONTENTS	vi
LIST OF FIGURES	viii
LIST OF TABLES	x
NOMENCLATURE	xi
INTRODUCTION	1
THEORY AND MATHEMATICAL MODEL	4
DESCRIPTION OF THE TEST RIG	5
Parameter Identification	6
Test seals	8
Fluid preswirl.....	9
Leakage flow.....	10
Test conditions	11
EXPERIMENTAL RESULTS	12
Baseline data	12
Test data uncertainty	12
COMPARISON BETWEEN CONSTANT CLEARANCE AND CONVERGENT- TAPERED HONEYCOMB ANNULAR GAS SEALS	14
Direct and cross-coupled stiffness	14
Direct and cross-coupled damping	16
Effective stiffness and effective damping.....	17
Seal leakage	18
EXPERIMENT VERSUS THEORETICAL PREDICTIONS	19
Direct and cross-coupled stiffness	19
Direct and cross-coupled damping	22
Effective stiffness and effective damping.....	22
Seal leakage	27
SUMMARY AND CONCLUSIONS	29
REFERENCES	31
APPENDIX A.....	34
APPENDIX B.....	35

VITA45

LIST OF FIGURES

FIGURE	Page
1 Typical rotor - annular seal configuration [15].....	1
2 Cross-sectional view of the test rig	5
3 Cross-section view of the preswirl ring [16]	10
4 Comparison of Experimental Direct and Cross-coupled Stiffness for CCHC ($q=0$) and CTHC $q=0.24$ with Zero Preswirl, $\omega = 20,200$ RPM, and $P_i = 69$ bar (1,000 psi).....	15
5 Comparison of Experimental Direct and Cross-coupled Damping for CCHC ($q=0$) and CTHC $q=0.24$ with Zero Preswirl, $\omega = 20,200$ RPM, and $P_i = 69$ bar (1,000 psi).....	16
6 Comparison of Experimental Effective Stiffness and Damping for CCHC ($q=0$) and CTHC $q=0.24$ with Zero Preswirl, $\omega = 20,200$ RPM, and $P_i = 69$ bar (1,000 psi).....	17
7 Comparison of Experimental Leakage for CCHC ($q=0$) and CTHC $q=0.24$ with Zero Preswirl, $\omega = 20,200$ RPM, and $P_i = 69$ bar (1,000 psi)	18
8 Experimental and Theoretical Direct and Cross-coupled Stiffness for CCHC ($q=0$) and CTHC $q=0.24$ with Zero Preswirl, $\omega = 20,200$ RPM, and $P_i = 69$ bar (1,000 psi).....	20
9 Experimental and Theoretical Direct and Cross-coupled Stiffness for CTHC $q = 0.386$ with Zero Preswirl, $\omega = 20,200$ RPM, and $P_i = 69$ bar (1,000 psi).....	21
10 Experimental and Theoretical Direct and Cross-coupled Damping for CCHC ($q=0$) and CTHC $q=0.24$ with Zero Preswirl, $\omega = 20,200$ RPM, and $P_i = 69$ bar (1,000 psi).....	23
11 Experimental and Theoretical Direct and Cross-coupled Damping for CTHC $q = 0.386$ with Zero Preswirl, $\omega = 20,200$ RPM, and $P_i = 69$ bar (1,000 psi).....	24

FIGURE	Page
12 Experimental and Theoretical Effective Stiffness and Damping for CCHC ($q=0$) and CTHC $q=0.24$ with Zero Preswirl, $\omega = 20,200$ RPM, and $P_i = 69$ bar (1,000 psi).....	25
13 Experimental and Theoretical Effective Stiffness and Damping for CTHC $q = 0.386$ with Zero Preswirl, $\omega = 20,200$ RPM, and $P_i = 69$ bar (1,000 psi)..	26
14 Experimental and Theoretical Leakage for CCHC ($q=0$) and CTHC $q=0.24$ with Zero Preswirl, $\omega = 20,200$ RPM, and $P_i = 69$ bar (1,000 psi).....	27
15 Experimental and Theoretical Leakage for CTHC $q=0.386$ with Zero Preswirl, $\omega = 20,200$ RPM, and $P_i = 69$ bar (1,000 psi)	28

LIST OF TABLES

TABLE		Page
1	Dimensions of the Seals	8
2	q Factors.....	9
3	Test Matrix	11
4	Static Parameter's Uncertainties.....	12
5	Exact Test Conditions	34
6	Zero Preswirl, PR = 30%, 10,200 rpm for $q = 0.24$	35
7	Zero Preswirl, PR = 30%, 15,200 rpm for $q = 0.24$	36
8	Zero Preswirl, PR = 30%, 20,200 rpm for $q = 0.24$	36
9	Zero Preswirl, PR = 40%, 10,200 rpm for $q = 0.24$	37
10	Zero Preswirl, PR = 40%, 15,200 rpm for $q = 0.24$	37
11	Zero Preswirl, PR = 40%, 20,200 rpm for $q = 0.24$	38
12	Zero Preswirl, PR = 46%, 10,200 rpm for $q = 0.24$	38
13	Zero Preswirl, PR = 46%, 15,200 rpm for $q = 0.24$	39
14	Zero Preswirl, PR = 46%, 20,200 rpm for $q = 0.24$	39
15	Zero Preswirl, PR = 20%, 10,200 rpm for $q = 0.386$	40
16	Zero Preswirl, PR = 20%, 15,200 rpm for $q = 0.386$	40
17	Zero Preswirl, PR = 20%, 20,200 rpm for $q = 0.386$	41
18	Zero Preswirl, PR = 30%, 10,200 rpm for $q = 0.386$	41
19	Zero Preswirl, PR = 30%, 15,200 rpm for $q = 0.386$	42
20	Zero Preswirl, PR = 30%, 20,200 rpm for $q = 0.386$	42
21	Zero Preswirl, PR = 40%, 10,200 rpm for $q = 0.386$	43
22	Zero Preswirl, PR = 40%, 15,200 rpm for $q = 0.386$	43
23	Zero Preswirl, PR = 40%, 20,200 rpm for $q = 0.386$	44

NOMENCLATURE

C_r	-	Radial Clearance	[L]
C_{ri}	-	Radial Inlet Clearance	[L]
C_{re}	-	Radial Exit Clearance	[L]
C	-	Direct Damping	[FT/L]
c	-	Cross-coupled Damping	[FT/L]
C_{ij}	-	Damping Coefficient	[FT/L]
C_{eff}	-	Effective Damping	[FT/L]
D_r	-	Rotor Diameter	[L]
f_s	-	Seal Reaction Force	[F]
g	-	Acceleration due to Gravity	[L/T ²]
H_{ij}	-	Impedance	[F/L]
H_w	-	Inches of Water	[L]
j	-	$\sqrt{-1}$	[-]
K	-	Direct Stiffness	[F/L]
k	-	Cross-coupled Stiffness	[F/L]
K_{ij}	-	Stiffness Coefficient	[F/L]
K_{eff}	-	Effective Stiffness	[F/L]
L	-	Seal Length	[L]
m_s	-	Stator Mass	[M]
N	-	Rpm	[1/T]
P	-	Pressure	[F/L ²]
P_i	-	Inlet Pressure	[F/L ²]
P_e	-	Exit Pressure	[F/L ²]
q	-	Taper-angle Seal Parameter	[-]
R_c	-	Gas Constant	[FL/(MT)]
\ddot{R}	-	Stator Acceleration Vector	[L/T ²]
T_i	-	Inlet Temperature	[Θ]
T_e	-	Exit Temperature	[Θ]

V_t	-	Inlet Tangential (Swirl) Velocity	[L/T]
X,Y	-	Displacement Directions	[L]
\dot{X}, \dot{Y}	-	Velocities	[L/T]
ΔP	-	Differential Pressure	[F/L ²]
\dot{m}	-	Mass Flow Rate	[M/T]
\dot{Q}	-	Volumetric Flow Rate	[L ³ /T]
ε	-	Eccentricity Ratio	[-]
γ	-	Gamma Factor	[-]
Ω	-	Excitation Frequency	[1/T]
ω	-	Running Speed	[1/T]

Abbreviations

CTHC	-	Convergent-Tapered Honeycomb Seals	[-]
PR	-	Pressure Ratio	[-]
PS	-	Preswirl Ratio	[-]
CCHC	-	Constant Clearance Honeycomb Seals	[-]

INTRODUCTION

Annular gas seals with roughness patterns are being used in compressors and turbines not only to control the leakage of the working fluid, but also to enhance rotordynamic stability. A typical honeycomb seal and rotor configuration is shown in Figure 1, where the direction of the rotor as well as the preswirl rotation is shown. Troubles have been encountered in some seals that become divergent during operation Cimatti et al [1]. To deal with this eventuality, some seals are being installed with converging flow. Converging flow paths are predicted to produce increased direct stiffness and decreased direct damping; however, data have only been published for convergent annular gas seals in terms of either leakage or rotordynamic coefficients to supply pressures up to 18 bar (250 psi), Dawson [2].

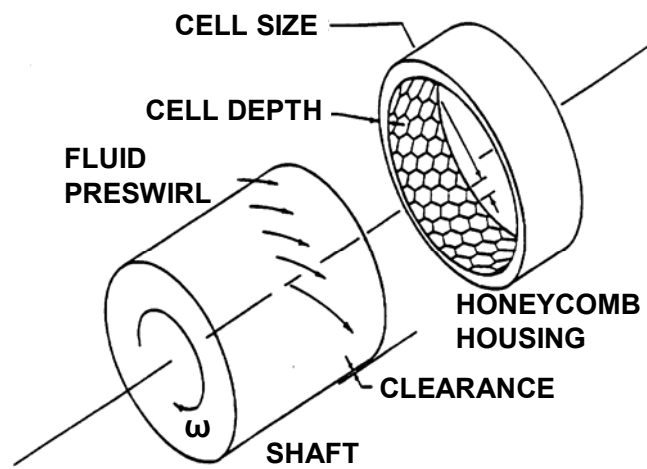


Figure 1 Typical rotor - annular seal configuration [15]

Nelson [3, 4] developed the initial analysis for rotordynamic coefficients of annular seals, using a “bulk-flow” model based on Hirs [5]. Additionally, he notes the effects of fluid pre-rotation and choked flow on the rotordynamic coefficients. His analysis technique is similar to Childs [6, 7], whereby a set of governing turbulent bulk flow equations are developed, and then a perturbation analysis is employed to obtain a set of zero-and first-order equations. Integration of the zeroth-order equations yields the leakage, and integration of the first-order equations yields the direct and cross-coupled coefficients. Nelson et al. [8] compare predicted and experimental rotordynamic coefficients of constant-clearance and convergent-tapered smooth seals. Their results verify the predictions by Nelson [3, 4] and Fleming [9, 10], that a gas path seal for which the inlet clearance is larger than the outlet clearance, will develop considerably higher direct stiffness than constant clearance seal designs. Nelson’s [3, 4] models gave reasonable results for smooth surfaces with surface roughness friction factors only; however, for honeycomb seals this model did not predict well measured rotordynamic coefficients.

Ha and Childs [11] proposed a two-control-volume model approach for honeycomb annular gas seal analysis by expanding Nelson’s model to account for radial transient flow into and out of the honeycomb cells. This effort led to the conclusion of frequency-dependent rotordynamic analysis by Kleynhans and Childs [12] for annular gas seals shown in Equation (1).

$$-\begin{Bmatrix} f_{sX} \\ f_{sY} \end{Bmatrix} = \begin{bmatrix} K(\Omega) & k(\Omega) \\ -k(\Omega) & K(\Omega) \end{bmatrix} \begin{Bmatrix} X \\ Y \end{Bmatrix} + \begin{bmatrix} C(\Omega) & c(\Omega) \\ -c(\Omega) & C(\Omega) \end{bmatrix} \begin{Bmatrix} \dot{X} \\ \dot{Y} \end{Bmatrix} \quad (1)$$

The direct stiffness and cross-coupled stiffness coefficients are represented by K and k respectively, and the direct damping and cross-coupled damping coefficients are represented by C and c respectively. All coefficients are functions of the excitation frequency (Ω). This model just applies for small motion about a centered position.

Childs, Elrod, and Hale [13] were the first to perform dynamic tests with honeycomb seals. The rotor was shaken at frequencies from 30 Hz to 75 Hz; this allowed the direct and cross-coupled stiffness and damping to be measured.

Dawson [2] tested two geometries of honeycomb seals with 114.3 mm bore and radial clearance of 0.2 mm from the test rotor. He demonstrated that the convergent tapered-bore seals exhibited significantly larger (73%) effective stiffness and had significantly less effective damping (71%) compared to the straight-bore honeycomb seals. He observed the effects of constant-clearance versus a convergent tapered-bore annular gas seals with inlet pressure ranged from 6.9 bar (100 psi) to 17.2 bar (250 psi), speeds up to 20,200 rpm, and for the back-pressure ratios 0.4 and 0.6. He also showed that the rotordynamic coefficients are frequency-dependent. The rotor was shaken at frequencies from 20 Hz to 300 Hz.

Weatherwax and Childs [14] tested a honeycomb-stator/smooth-rotor annular seal with 115 mm bore, for eccentricity ratios out to 0.5 with air at a supply pressure of 69 bar (1,000 psi) and speeds up to 20,200 rpm at frequencies from 20 Hz to 300 Hz, in order to examine the effect of eccentricity. Tests were conducted for the back-pressure ratios 0.15, 0.35, and 0.5. They found that the eccentricity of the rotor did not affect either leakage or the rotordynamic coefficients even when the rotor was displaced up to 50% of the clearance.

Sprowl [15] tested a constant-clearance honeycomb seal at supply pressure up to 70 bar (1015 psi) with 114.7 mm bore and radial clearance of 0.2 mm from the test rotor. The rotor was shaken at frequencies from 20 Hz to 300 Hz, and tests were conducted for the back-pressure ratios 0.15, 0.35, and 0.5 with speeds up to 20,200 rpm. He found that his seals were not very sensitive to fluid preswirl under the conditions of his testing.

THEORY AND MATHEMATICAL MODEL

The Laplace transform model from Kleynhans and Childs [12] for small motion about a centered position, shown in Equation (2), was used to model the reaction forces of the seal.

$$-\begin{Bmatrix} f_{sX}(s) \\ f_{sY}(s) \end{Bmatrix} = \begin{bmatrix} \mathbf{G} & \mathbf{E} \\ -\mathbf{E} & \mathbf{G} \end{bmatrix} \begin{Bmatrix} \mathbf{X}(s) \\ \mathbf{Y}(s) \end{Bmatrix} \quad (2)$$

Equation (2) is presented in the Laplace domain, where s is the Laplace domain variable, f_s is the reaction force vector, and $\mathbf{X}(s)$ and $\mathbf{Y}(s)$ represent the Laplace domain components of the relative displacement between the rotor and stator. This model can be used to model seals that have rotordynamic coefficients that are affected greatly by the excitation frequency. Equation (3) includes the frequency dependent stiffness and damping coefficients in the seal model.

$$-\begin{Bmatrix} f_{sX} \\ f_{sY} \end{Bmatrix} = \begin{bmatrix} K(\Omega) & k(\Omega) \\ -k(\Omega) & K(\Omega) \end{bmatrix} \begin{Bmatrix} X \\ Y \end{Bmatrix} + \begin{bmatrix} C(\Omega) & c(\Omega) \\ -c(\Omega) & C(\Omega) \end{bmatrix} \begin{Bmatrix} \dot{X} \\ \dot{Y} \end{Bmatrix} \quad (3)$$

The two models are related by the following equations.

$$\begin{aligned} \mathbf{G}(j\Omega) &= \mathbf{K}(\Omega) + j\mathbf{C}(\Omega) \\ \mathbf{E}(j\Omega) &= k(\Omega) + jc(\Omega) \end{aligned} \quad , \quad (4)$$

where $j = \sqrt{-1}$.

Effective stiffness and effective damping are two other coefficients that are very useful in comparing the rotordynamic performance of seals. These coefficients are shown in Equations (5) and (6).

$$K_{eff}(\Omega) = K(\Omega) + c(\Omega)\Omega \quad (5)$$

$$C_{eff} = C(\Omega) - \frac{k(\Omega)}{\Omega} \quad (6)$$

DESCRIPTION OF THE TEST RIG

The test rig has been explained in numerous previous theses – Dawson [2] and Wade [16] – and several publications – Dawson et al. [17] and Weatherwax and Childs [14]. Consequently, it will be shortly reviewed here.

Figure 2 illustrates the current air seal test rig. Test air enters the seal housing between two identical seals and exits axially across the seals. Downstream exit labyrinths hold back pressure on the seals. Flow can be withdrawn from the annulus between the exit of the test seal and the inlet to the labyrinths to control the pressure ratio across the seal independently from the supply pressure. The pressure ratio is defined as the seal exit pressure divided by the seal inlet pressure.

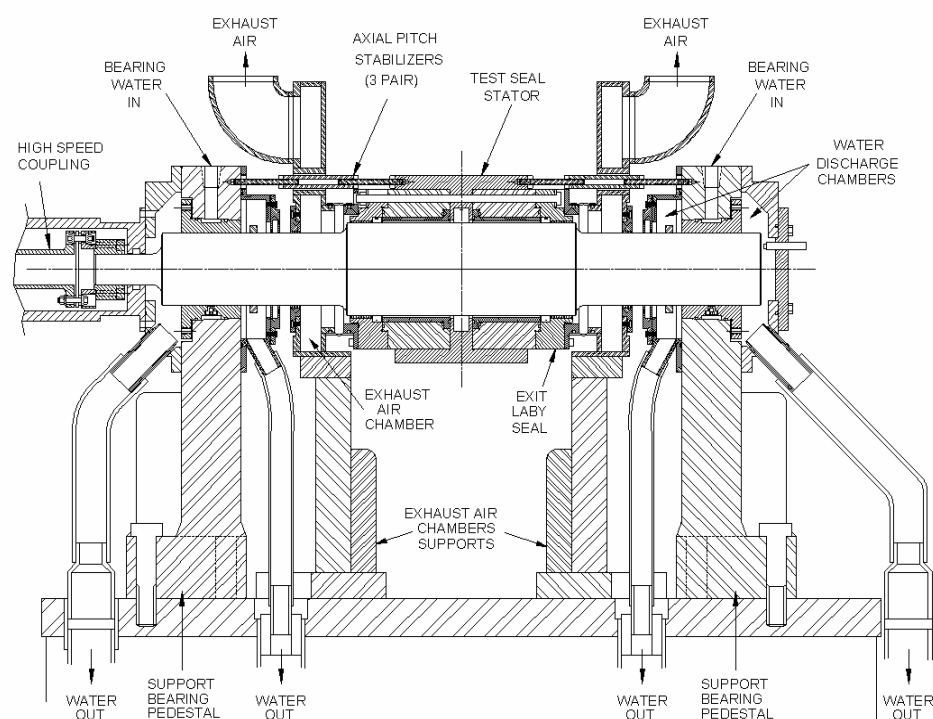


Figure 2 Cross-sectional view of the test rig [2]

The test rig was originally designed to test high-speed hydrostatic bearings. A complete description of the original test stand configuration is included in Childs and

Hale [18]. The rig was later altered to accommodate the testing of gas seals. Dawson [2] describes how the test rig was altered to allow the testing of annular gas seals with inlet pressure of up to 17.2 bar (250 psi). Later, the test rig was modified again to allow testing of annular gas seals at much higher inlet pressures of up to 84 bar (1,235 psi). Weatherwax and Childs [14], explain how the test rig was altered to enable this high pressure testing. The test rotor can spin up to 29,000 RPM. The backpressure can be regulated to achieve different pressure drops across the test seals.

The testing is conducted using two rotors that are 114.3 mm (4.500 in) and 114.5 mm (4.508 in) respectively; this enables the same seals to be tested at two different clearances. The rotors are supported on hydrostatic bearings as shown in Figure 2. The test seals are aligned with the rotor, and the seals are restrained in the axial direction using six pitch stabilizers. Two orthogonally located hydraulic shakers control the radial movement of the stator. The two hydraulic shakers are both located at 45 degrees from the vertical, on the upper side of the stator.

Parameter identification

The stator is excited in two orthogonal directions as stated before. The equation for the stator's motion is,

$$\begin{Bmatrix} f_X \\ f_Y \end{Bmatrix} - \begin{Bmatrix} m_s \ddot{R}_{sX} \\ m_s \ddot{R}_{sY} \end{Bmatrix} = - \begin{Bmatrix} f_{sX} \\ f_{sY} \end{Bmatrix}, \quad (7)$$

where f is the measured excitation force, f_s is the seal reaction force, \ddot{R}_s is the measured acceleration of the stator, and m_s is the stator mass. Restating Equation (7) in the frequency domain yields,

$$\begin{Bmatrix} F_X - m_s A_X \\ F_Y - m_s A_Y \end{Bmatrix} = - \begin{bmatrix} H_{XX} & H_{XY} \\ H_{YX} & H_{YY} \end{bmatrix} \begin{Bmatrix} D_X \\ D_Y \end{Bmatrix} \quad (8)$$

where \mathbf{F} and \mathbf{A} are complex force and acceleration vectors expressed in the frequency domain, and the dynamic stiffness coefficient matrix defines the seal reaction forces. There are four unknowns \mathbf{H}_{XX} , \mathbf{H}_{XY} , \mathbf{H}_{YX} , and \mathbf{H}_{YY} .

To solve for the four unknowns the stator is shaken in orthogonal, X and Y directions. By shaking in two orthogonal directions four independent equations are obtained with four unknowns given by Equation (9).

$$\begin{bmatrix} \mathbf{F}_{XX} - m_s \mathbf{A}_{XX} & \mathbf{F}_{XY} - m_s \mathbf{A}_{XY} \\ \mathbf{F}_{XX} - m_s \mathbf{A}_{XX} & \mathbf{F}_{XY} - m_s \mathbf{A}_{XY} \end{bmatrix} = - \begin{bmatrix} \mathbf{H}_{XX} & \mathbf{H}_{XY} \\ \mathbf{H}_{YX} & \mathbf{H}_{YY} \end{bmatrix} \begin{bmatrix} \mathbf{D}_{XX} & \mathbf{D}_{XY} \\ \mathbf{D}_{YX} & \mathbf{D}_{YY} \end{bmatrix} \quad (9)$$

Equation (9) is valid for small motion about a position and has been verified by previous tests. The stiffness and damping terms are found directly from the impedances.

$$K(\Omega) = \text{Re}(\mathbf{H}_{ii}(\Omega)) \quad (10)$$

$$k(\Omega) = \text{Re}(\mathbf{H}_{ij}(\Omega)) \quad (11)$$

$$C(\Omega) = \frac{\text{Im}(\mathbf{H}_{ii}(\Omega))}{\Omega} \quad (12)$$

$$c(\Omega) = \frac{\text{Im}(\mathbf{H}_{ij}(\Omega))}{\Omega} \quad (13)$$

Some of the DESCRIPTION OF THE TEST RIG and EXPERIMENTAL RESULTS sections are taken from Wade [16], and Seifert [19]

Test seals

The testing was performed on a convergent tapered honeycomb annular gas seal with an inlet pressure of 69 bar (1,000 psi). The significant dimensions of the seal are listed in Table 1.

Table 1 Dimensions of the Seals

Seal Length	85.725 mm	3.375 in
Diameter of the Seal at Entrance	114.968 mm	4.5263 in
Diameter of the Seal at Exit	114.709 mm	4.5161 in
Cell Width	0.79 mm	1/32 in
Cell Depth	3.175 mm	0.125 in
Gamma factor (γ)	0.885	

Gamma is the ratio of the area of the holes to the area of the inner surface of the seal. The seals tested have a gamma factor of 0.885; therefore, 88.5% of the inner surface area is taken up by holes.

This seal geometry was tested by Dawson et al [17] with constant clearance (diameter of the seal of 114.3 mm), with 0.2 mm radial clearance, for three seal inlet pressures, 6.9 bar (100 psi), 12.1 bar (175 psi), and 17.2 bar (250 psi). Sprowl [15] also tested a constant-clearance honeycomb seal with the same geometry, but this time with an inlet pressure of approximately 69 bar (1,000 psi). Their prior data will serve as a reference in terms of a convergent taper's impact on stiffness, damping, and leakage for Sprowl's [15] seals, and the effect when increasing the seal inlet pressure for Childs and Dawson [17].

Two exit radial clearances, C_{re} , of 0.1 and 0.2 mm were used. An inlet radial clearance, C_{ri} , was selected based on predictions from the two-control-volume theory by Kleynhans and Childs to yield a compromise between increasing direct stiffness while decreasing damping. The q factor, which is just a simple way to quantify taper is defined by Equation (14). Therefore, three taper-angle seal parameters were defined

using the selected inlet radial clearance shows in Table 2, and the two exit radial clearances mentioned before. The three q factors are shown in Table 2.

$$q = \frac{C_{ri} - C_{re}}{C_{ri} + C_{re}} \quad (14)$$

Table 2 q Factors

Diameter of the Rotor	Radial Inlet Clearance	Radial Exit Clearance	q Factor
114.3 mm (4.5 in)	0.204 mm (8.05 mils)	0.204 mm (8.05 mils)	0
114.3 mm (4.5 in)	0.334 mm (13.15 mils)	0.204 mm (8.05 mils)	0.24
114.503 mm (4.508 in)	0.233 mm (9.15 mils)	0.103 mm (4.05 mils)	0.386

Fluid preswirl

Fluid preswirl is defined as the fluid's inlet circumferential velocity divided by the rotor's surface speed, Equation (15).

$$Ratio_{pre-swirl} = \frac{V_t \cdot 60}{\pi \cdot N \cdot D_r} \quad (15)$$

Tests were at near zero preswirl, simulating a balance-piston or division-wall seal with an effective swirl brake. Figure 3 shows a cross-section view of the zero preswirl ring.

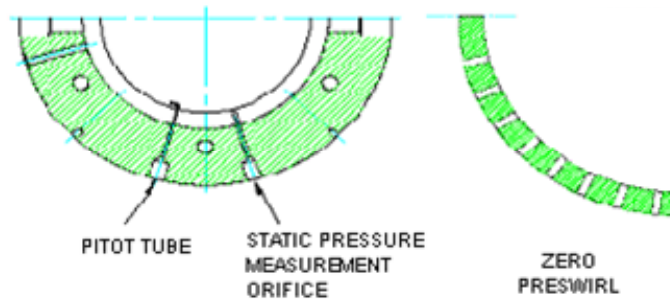


Figure 3 Cross-section view of the preswirl ring [16]

The high-pressure air is fed into the inlet annulus and then flows through the preswirl ring before entering the test seals. The preswirl ring in the inlet annulus directs the air circumferentially. The zero preswirl ring has holes that are radial, injecting the air radially onto the rotor.

Leakage flow

All annular seals allow a certain amount of leakage to occur. Leakage depends on many factors, but the main factors in determining how much mass flow a given annular gas seal will allow in a given situation are, the pressure drop across the seal, the radial clearance between the rotor and the seal, the length of the seal, and the relative roughness of the seal and rotor surfaces.

The test rig measures the volumetric flow rate of air that flows through the rig by a turbine style flow meter up stream of the test seals. The flow meter is located between the inlet control valve and the inlet annulus of the test stator and measures the total flow through both seals. Since the seals are physically as close to identical as possible, and the pressure drop across both seals is measured and found to be approximately the same, the flow is assumed to be split evenly between each seal.

The temperature and pressure of the air passing through the flow meter are also measured and used to convert from volumetric flow rate to mass flow rate. As the test is running, the volumetric flow rate, the temperature, and the pressure of the air are recorded five times before a shake test is run. These five samples are recorded while

the test rig is operating in a steady state condition. The five data points are then averaged, and the average value is what has been reported.

Test conditions

The seals were tested in a variety of conditions, two different rotors, three pressure ratios and three rotor speeds with a total of 18 different test conditions. The test matrix is presented in Table 3.

The test rig does not control the temperature of the inlet air. Since the temperature of the incoming air was not controllable, it was recorded, to be used later to make corrections for air density.

Table 3 Test Matrix

Inlet Pressure	Pre-Swirl	q Factor	Pressure Ratio	Rotor Speed
69 bar (1,000 psi)	Zero	0.24	0.30, 0.40, 0.46	10,200 RPM
			0.30, 0.40, 0.46	15,200 RPM
			0.30, 0.40, 0.46	20,200 RPM
		0.386	0.20, 0.30, 0.40	10,200 RPM
			0.20, 0.30, 0.40	15,200 RPM
			0.20, 0.30, 0.40	20,200 RPM

EXPERIMENTAL RESULTS

Baseline data

To account for the stiffness and damping that are not produced by the test seals, baseline data are measured. The baseline data are obtained by assembling the test rig without seals in the test stator. The stator is pressurized, and the stator is shaken with the rotor spinning and data recorded. This step is taken to measure the forces that result from the exit labyrinth seals and the stiffness and damping of the stator assembly. The rotordynamic coefficients are obtained by subtracting the baseline real and imaginary impedances from the corresponding real and imaginary impedances produced with the test seals installed.

Test data uncertainty

There is some uncertainty with any measurement. With these experiments, there is uncertainty in the measurements of force, acceleration, pressure, temperature, and rotor speed. Kurtin et al. [20] performed uncertainty analysis for the static coefficients of the test rig. The uncertainties are presented in Table 4.

Table 4 Static Parameter's Uncertainties

Shaft Speed	Pressure	Flow Rate	Eccentricity Ratio
(N)	(P)	(\dot{Q})	(ε)
10 RPM	3.747 kPa	0.177 L/min	0.005

To obtain an uncertainty value for the impedances, a single dynamic test was repeated ten times. The uncertainty of the impedances was found in this manner for each test. During testing, the 15,200 RPM rotor speed, tests were repeated ten times. The data were then reduced to calculate the stiffness and damping terms. The

standard deviation of each term at the discrete frequencies is then calculated. The standard deviation of the term is plotted as uncertainty bars on the data graphs.

Uncertainty data were taken in the same manner for the baseline data. All of the data that are reported in this thesis combine the baseline and test uncertainties. Equation (16) shows how the uncertainties are combined.

$$U_{total} = \sqrt{U_{Baseline}^2 + U_{Test_data}^2} \quad (16)$$

COMPARISON BETWEEN CONSTANT CLEARANCE AND CONVERGENT-TAPERED HONEYCOMB ANNULAR GAS SEALS

One of the main goals of this research was to compare the characteristics of constant clearance seals to the characteristics of convergent-tapered seals. All data were taken at 69 bar (1,000 psi). The seals used for comparison are constant clearance honeycomb seals from Sprowl [15]. The constant clearance honeycomb seals will be denoted as CCHC, and the convergent-tapered honeycomb seals as CTHC. The CCHC were tested with the smaller rotor, 0.2 mm (8 mils) constant radial-clearance $q=0$, while the CTHC were tested at two different radial-clearance conditions as explained before. It is important to recall that the CCHC ($q=0$) and the CTHC $q=0.24$ were tested with the same rotor diameter that was 114.3 mm (4.500 in), and the CTHC $q=0.386$ were tested with a different rotor diameter 114.5 mm (4.508 in). Therefore, just the CCHC ($q=0$) and the CTHC $q=0.24$ were used for comparison.

The data presented is for zero pre-swirl, the top speed, and for the pressure ratio that is closest to 0.5 for each testing condition. The exact testing pressure ratio were 0.5 for the CCHC ($q=0$), and 0.46 for the CTHC $q=0.24$.

Direct and cross-coupled stiffness

This section considers the effect of the different test conditions on direct and cross-coupled stiffness. The direct and cross-coupled stiffness comes from the real part of the impedance, as shown in Equations (10) and (11). Figure 4 shows the direct and cross-coupled stiffness for each test condition at 20,200 rpm. Notice that the CTHC $q=0.24$ produced higher direct stiffness coefficients at all frequencies than CCHC ($q=0$), eliminating the possibility of having negative static stiffness when obtained with CCHC ($q=0$). Also, for the cross-coupled stiffness CTHC $q=0.24$ produced higher cross-coupled stiffness coefficients at all frequencies than CCHC ($q=0$), especially at lower frequencies.

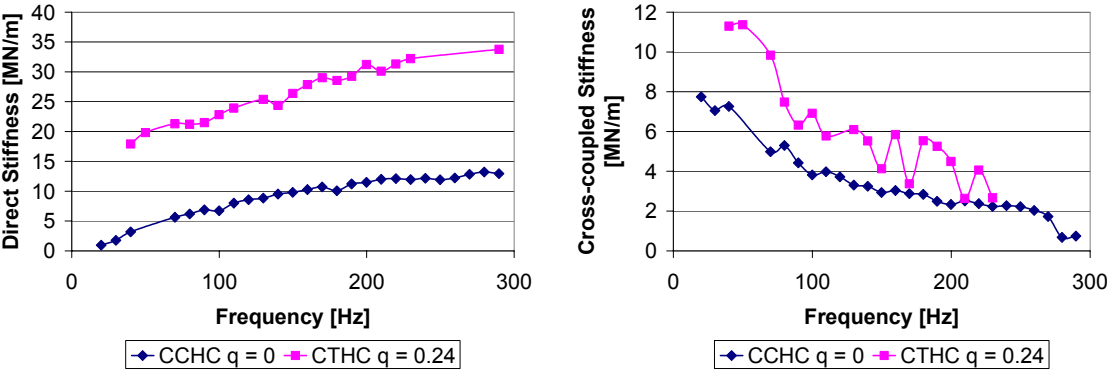


Figure 4 Comparison of Experimental Direct and Cross-coupled Stiffness for CCHC ($q=0$) and CTHC $q=0.24$ with Zero Preswirl, $\omega = 20,200$ RPM, and $P_i = 69$ bar (1,000 psi)

Direct and cross-coupled damping

This section examines the effect of the different test conditions on direct and cross-coupled damping. As shown in Equations (12) and (13), the direct and cross-coupled damping comes from the imaginary part of the impedances. Figure 5 illustrates the behavior of the direct and cross-coupled damping coefficients that were measured for each test condition at 20,200 rpm. Observe that CTHC $q = 0.24$ shows larger direct damping coefficients than CCHC ($q = 0$) except at lower frequencies. For the cross-coupled damping, CTHC $q = 0.24$ has also larger magnitude of the coefficients than CCHC ($q = 0$), especially at lower frequencies. These results are unexpected because normally a taper seal will decrease damping in comparison to a constant clearance seal tested at the same conditions.

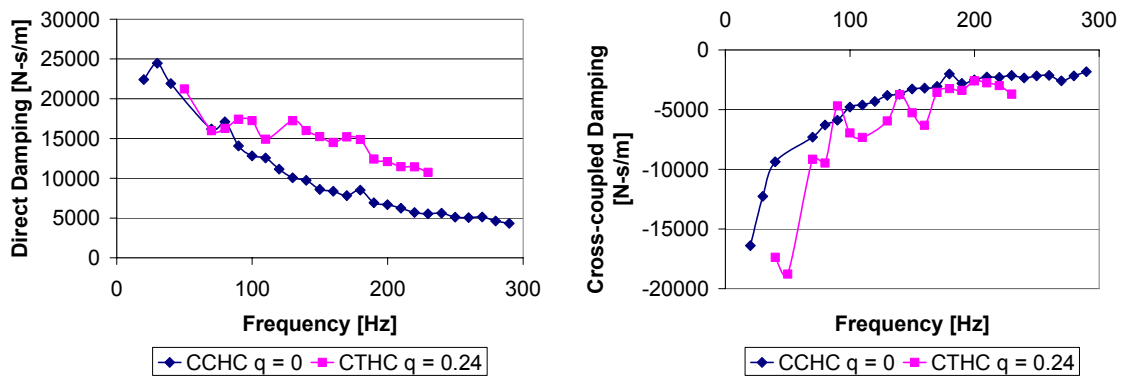


Figure 5 Comparison of Experimental Direct and Cross-coupled Damping for CCHC ($q = 0$) and CTHC $q = 0.24$ with Zero Preswirl, $\omega = 20,200$ RPM, and

$P_i = 69$ bar (1,000 psi)

Effective stiffness and effective damping

Effective stiffness is the effective centering force of the system. The formula for effective stiffness and damping are given in Equations (5) and (6). Effective damping is one of the best indicators in determining the stability of a roughened stator annular gas seal. The frequency at which it changes sign is called the cross-over frequency. In applications, this frequency needs to be lower than the rotor-system's first natural frequency. Otherwise, the seal will be highly destabilizing instead of highly stabilizing. From a rotordynamics viewpoint, we would like to decrease the cross-over frequency and increase effective damping. This section will present the taper's impact on effective stiffness and damping. Figure 6 shows the same behavior for effective stiffness with respect to direct stiffness; that is CTHC $q = 0.24$ produced higher effective stiffness coefficients at all frequencies than CCHC ($q = 0$). Notice that CTHC $q = 0.24$ eliminates the negative static stiffness obtained with CCHC ($q = 0$). For the effective damping, observe that the taper on the seals does increase the magnitude of the coefficients at all frequencies, since CTHC $q = 0.24$ has larger coefficients than CCHC ($q = 0$) before and after the cross-over frequency. In addition, it is very important to notice that CTHC $q = 0.24$ increase the cross-over frequency.

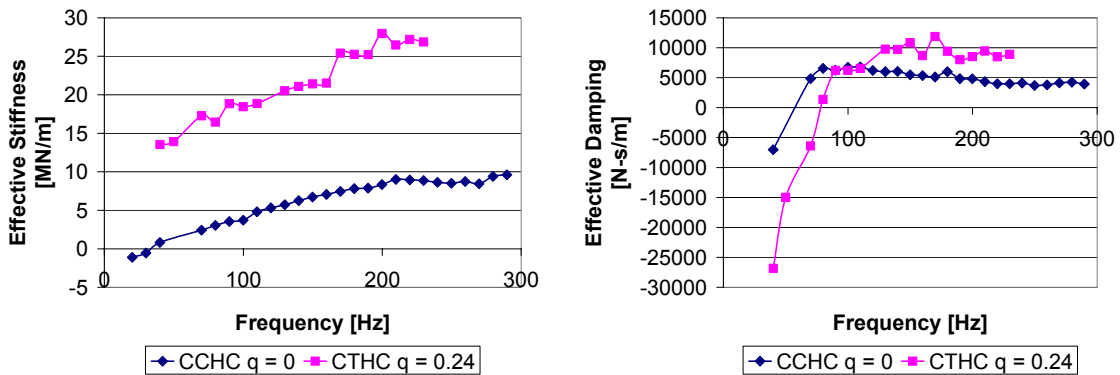


Figure 6 Comparison of Experimental Effective Stiffness and Damping for CCHC ($q=0$) and CTHC $q=0.24$ with Zero Preswirl, $\omega = 20,200$ RPM, and $P_1 = 69$ bar (1,000 psi)

Seal leakage

Figure 7 shows leakage versus pressure ratio for all test conditions at 20,200 rpm rotor speed. The data show that pressure ratio has some effect on leakage for all cases. Notice that CTHC $q = 0.24$ have approximately 20 percent more leakage than CCHC ($q = 0$) for all pressure ratios. This means that leakage coefficients increase with taper.

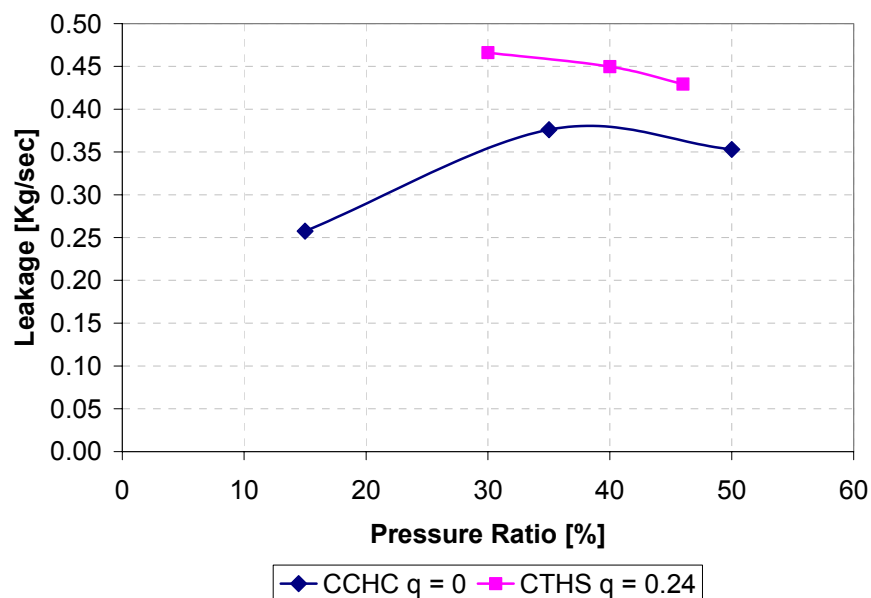


Figure 7 Comparison of Experimental Leakage for CCHC ($q = 0$) and CTHC $q = 0.24$ with Zero Preswirl, $\omega = 20,200$ RPM, and $P_i = 69$ bar (1,000 psi)

EXPERIMENT VERSUS THEORETICAL PREDICTIONS

Another main goal of this testing was to evaluate how well the two-control-volume theory by Kleynhans and Childs model predicts the static and dynamic characteristics of a convergent-tapered honeycomb seals in comparison with constant clearance seals. The constant clearance honeycomb seals data for comparison are from Sprowl [15]. This section will compare the experimental results with those predicted by the two-control-volume model. The experimental results contain uncertainty bars that result from the dynamic uncertainty described earlier. The error bars represent one standard deviation. The data presented is for zero pre-swirl, the top speed, and for the pressure ratio that is closest to 0.5 for each testing condition.

Direct and cross-coupled stiffness

Figures 8 and 9 present direct and cross-coupled stiffness versus excitation frequency. The test data points have uncertainty bars and the theory data are lines. The two-control-volume model does an excellent job predicting the direct stiffness coefficients for the CCHC ($q = 0$). For CTHC $q = 0.24$ the two-control-volume model under-predicts the direct stiffness at all frequencies, especially at high frequencies; however, for CTHC $q = 0.386$ the two-control-volume model over-predicts the direct stiffness at low frequencies (below 50 Hz) while under-predicts the coefficients for the rest of the frequencies. With respect to the cross-coupled stiffness, theory does a very good prediction for all tested seals for frequencies above 100Hz, especially for CCHC ($q = 0$) and CTHC $q = 0.386$. For frequencies below 100Hz the theory data under-predicts the cross-coupled coefficients for all cases.

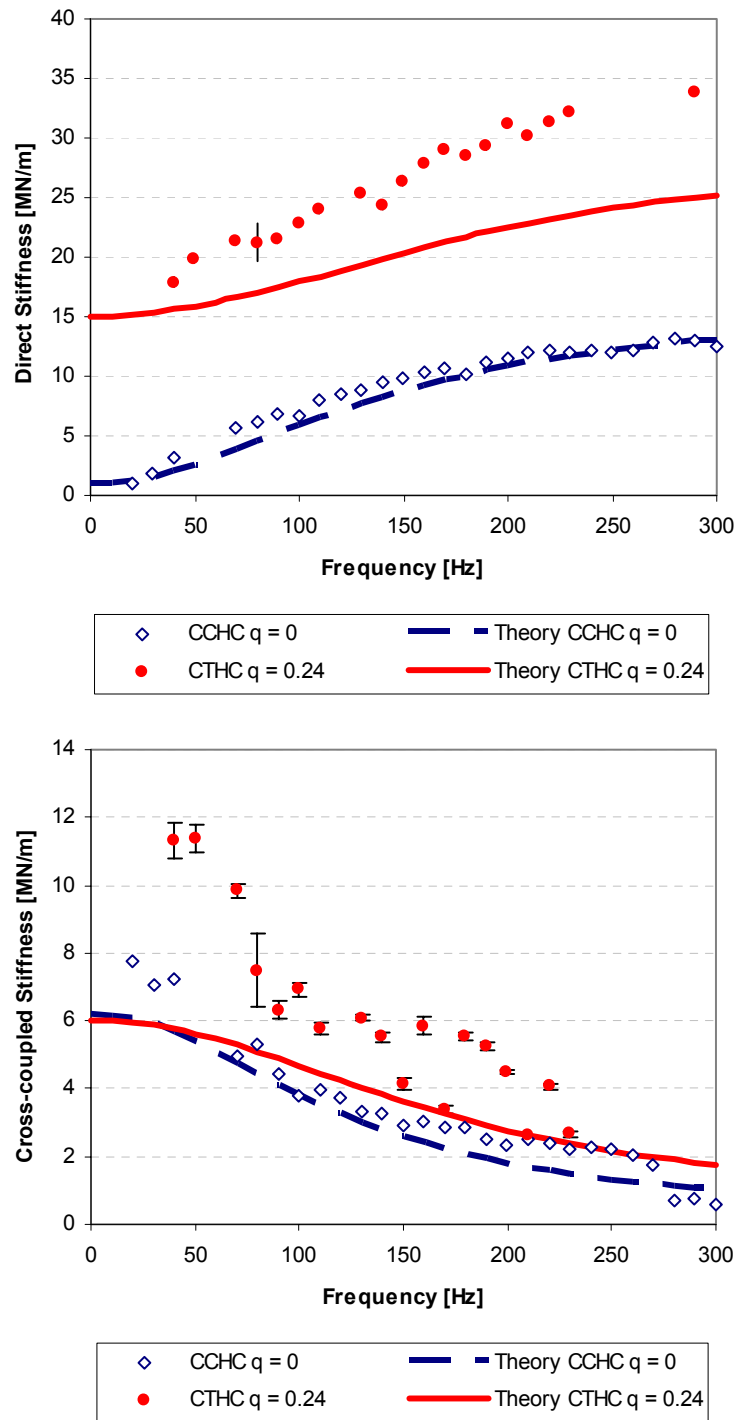


Figure 8 Experimental and Theoretical Direct and Cross-coupled Stiffness for CCHC ($q=0$) and CTHC $q=0.24$ with Zero Preswirl, $\omega = 20,200$ RPM, and $P_i = 69$ bar (1,000 psi)

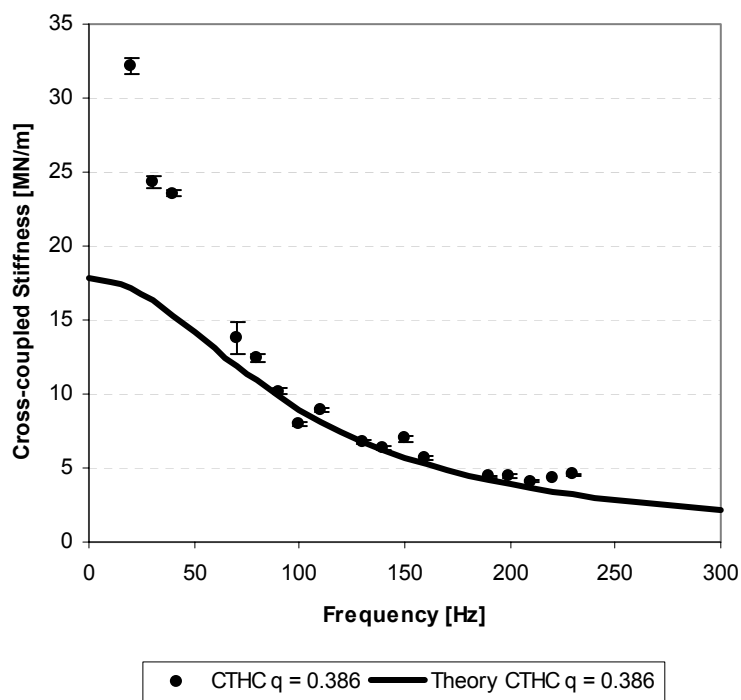
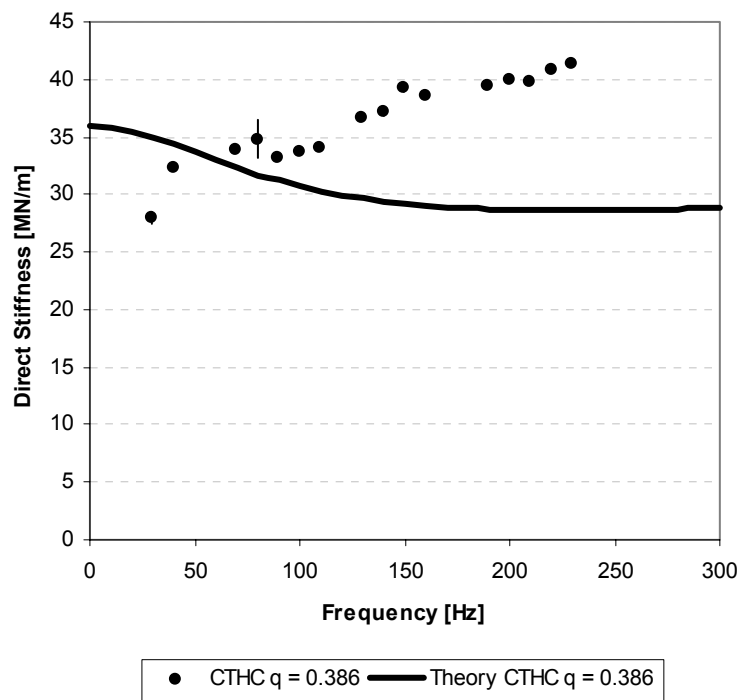


Figure 9 Experimental and Theoretical Direct and Cross-coupled Stiffness for CTHC $q = 0.386$ with Zero Preswirl, $\omega = 20,200$ RPM, and $P_i = 69$ bar (1,000 psi)

Direct and cross-coupled damping

Figures 10 and 11 present direct and cross-coupled damping versus excitation frequency. The test data points have uncertainty bars and the theory data are lines. The two-control-volume model under-predicts the direct damping at all frequencies for all tested seals, especially at low frequencies. For the CTHC's the theory becomes more accurate with $q = 0.386$. For the cross-coupled damping, the two-control-volume model does a very good prediction for all tested seals for frequencies above 150Hz. For frequencies below 150Hz the theory data under-predicts the magnitude of the cross-coupled damping except for $q = 0.386$ which over-predicts it.

Effective stiffness and effective damping

Figures 12 and 13 present effective stiffness and damping versus excitation frequency. The test data points have uncertainty bars and the theory data are lines. The two-control-volume model over-predicts slightly the effective stiffness coefficients at low frequencies for CCHC ($q=0$) and CTHC $q = 0.24$. For the CTHC $q = 0.386$ the two-control-volume model does not do a very good job at low frequencies. For the rest of the frequencies theory under-predicts the effective stiffness for all tested seals except for CCHC ($q=0$), which theory over-predicts again the coefficients at high frequencies. Once more, the two-control-volume model does a better prediction for CCHC ($q=0$) at all frequencies. For the effective damping the theory is very well predicted for CCHC ($q=0$). For CTHC $q = 0.24$ the theory under-predicts the magnitude of the effective damping at all frequencies. However, the cross-over frequency is predicted very well. For CTHC $q = 0.386$ the two-control-volume model does not predicts the cross-over frequency; nevertheless, it does predicts well the trend.

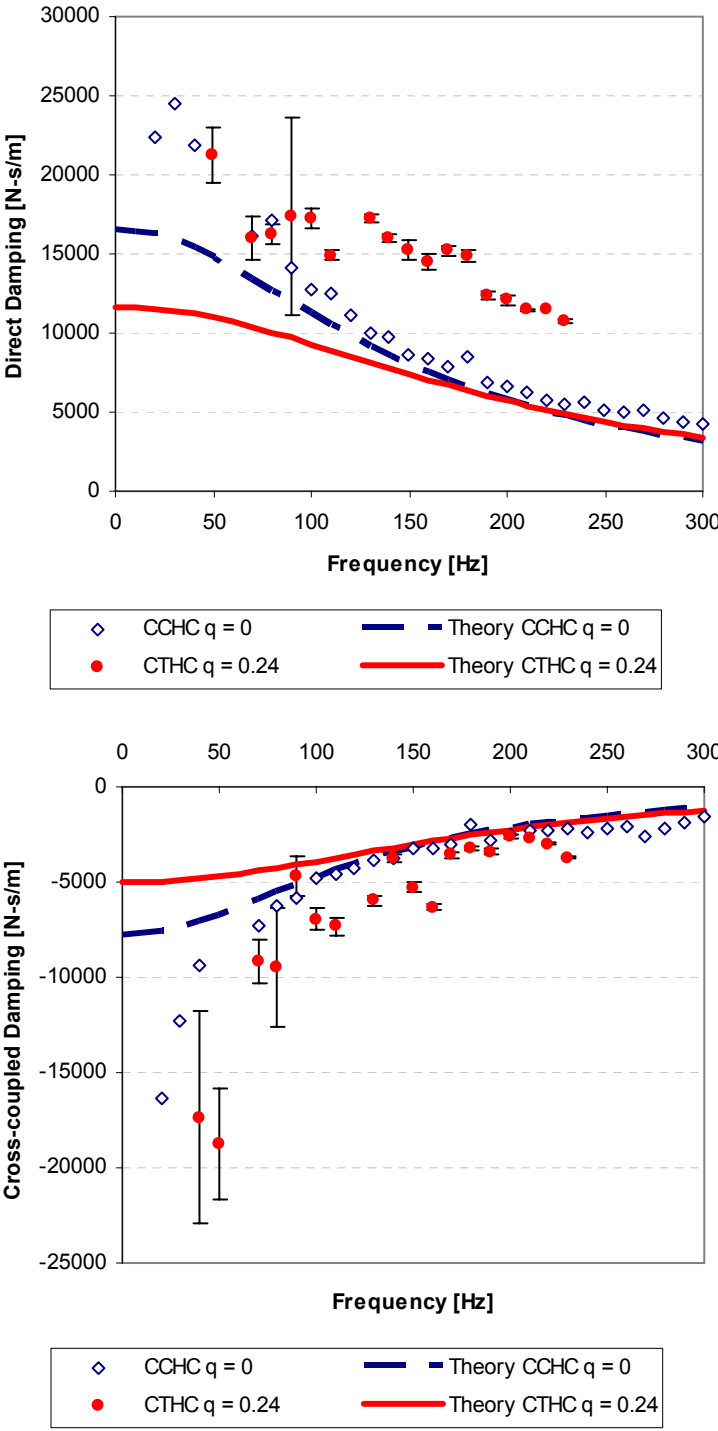


Figure 10 Experimental and Theoretical Direct and Cross-coupled Damping for CCHC ($q=0$) and CTHC $q=0.24$ with Zero Preswirl, $\omega = 20,200$ RPM, and $P_i = 69$ bar (1,000 psi)

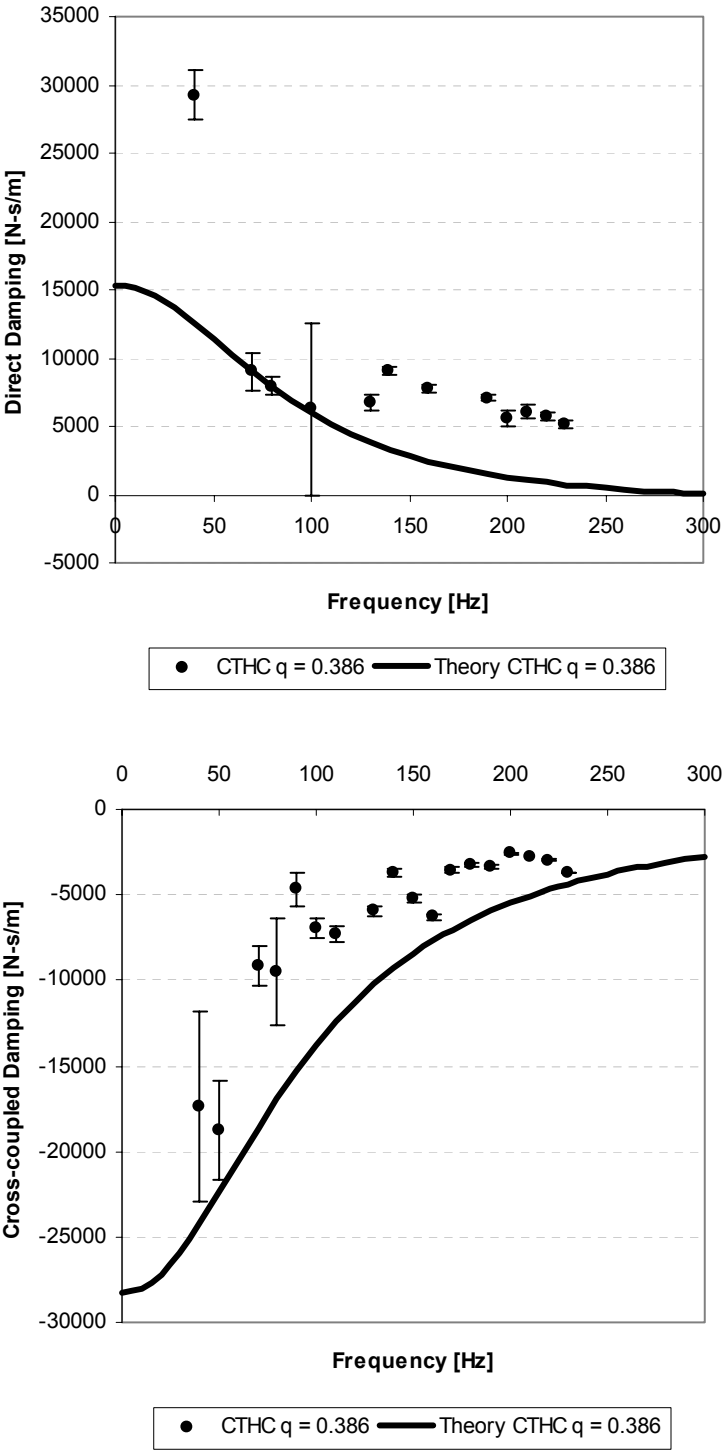


Figure 11 Experimental and Theoretical Direct and Cross-coupled Damping for CTHC $q = 0.386$ with Zero Preswirl, $\omega = 20,200$ RPM, and $P_i = 69$ bar (1,000 psi)

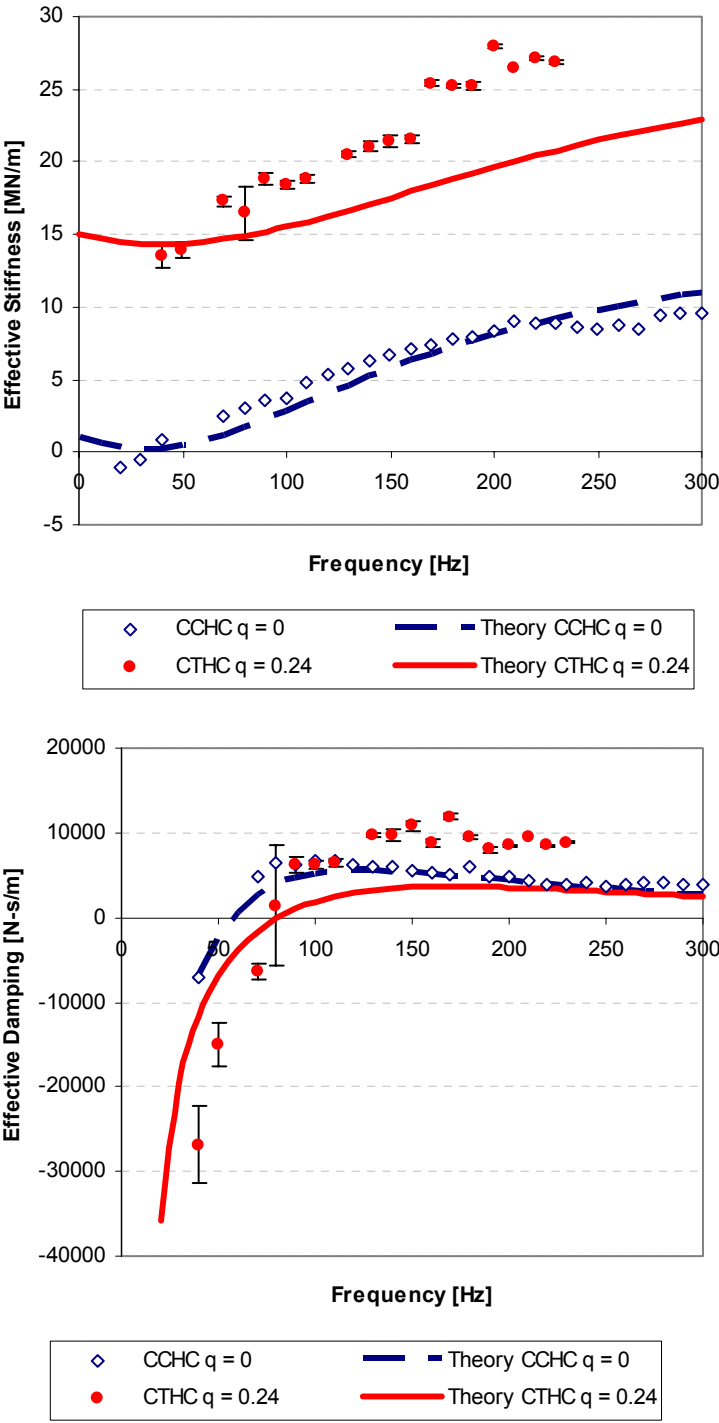


Figure 12 Experimental and Theoretical Effective Stiffness and Damping for CCHC ($q = 0$) and CTHC $q = 0.24$ with Zero Preswirl, $\omega = 20,200$ RPM, and $P_i = 69$ bar (1,000 psi)

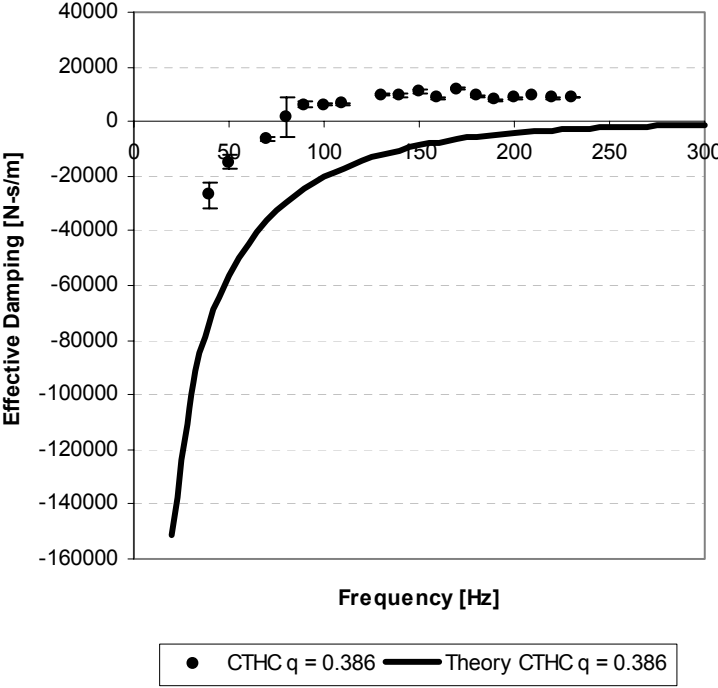
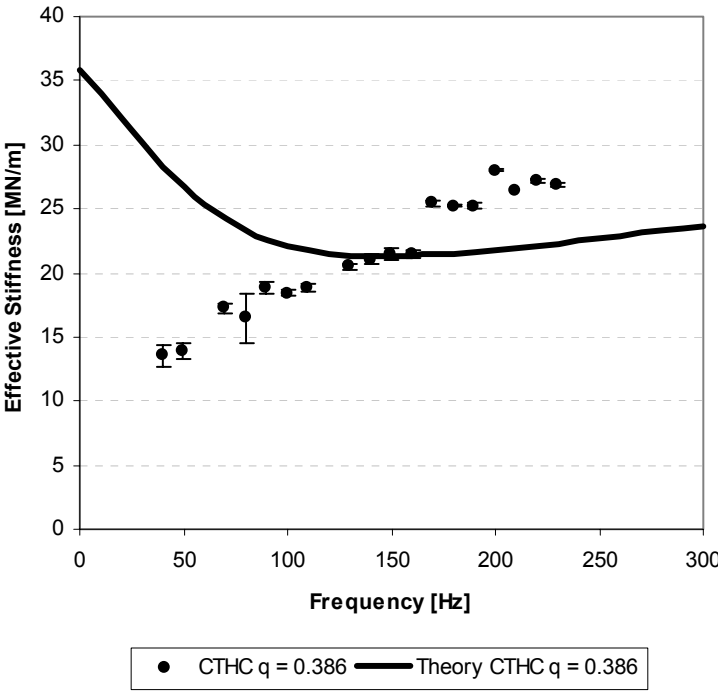


Figure 13 Experimental and Theoretical Effective Stiffness and Damping for CTHC $q = 0.386$ with Zero Preswirl, $\omega = 20,200$ RPM, and $P_i = 69$ bar (1,000 psi)

Seal leakage

Figures 14 and 15 present leakage versus pressure ratio for all test conditions at 20,200 rpm rotor speed. The two-control-volume model over-predicts the leakage coefficients for CCHC ($q=0$) between 14-18 percent, and for CTHC $q = 0.24$ between 12-19 percent. The over-prediction gets larger with increasing pressure ratio. Conversely, the two-control-volume model predicts very well the leakage for CTHC $q = 0.386$ because the under-prediction is less than 2 percent for all pressure ratios.

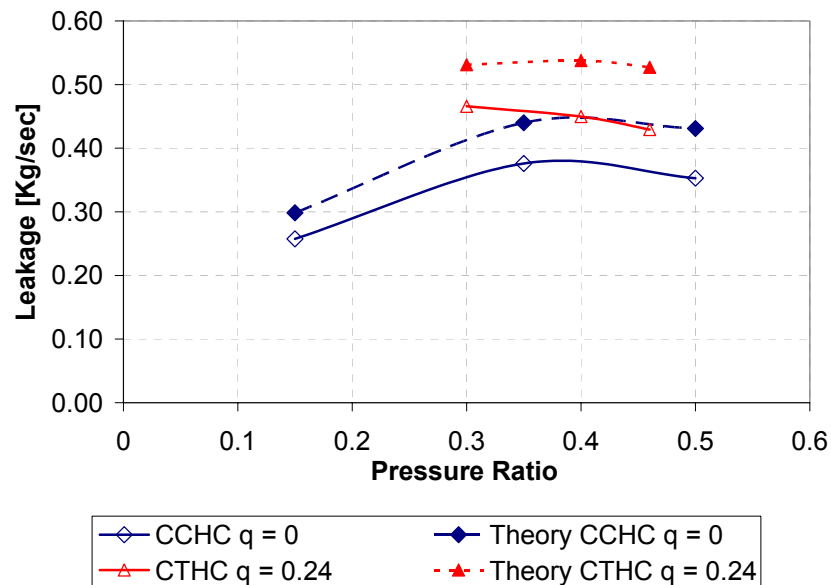


Figure 14 Experimental and Theoretical Leakage for CCHC ($q=0$) and CTHC $q=0.24$ with Zero Preswirl, $\omega = 20,200$ RPM, and $P_i = 69$ bar (1,000 psi)

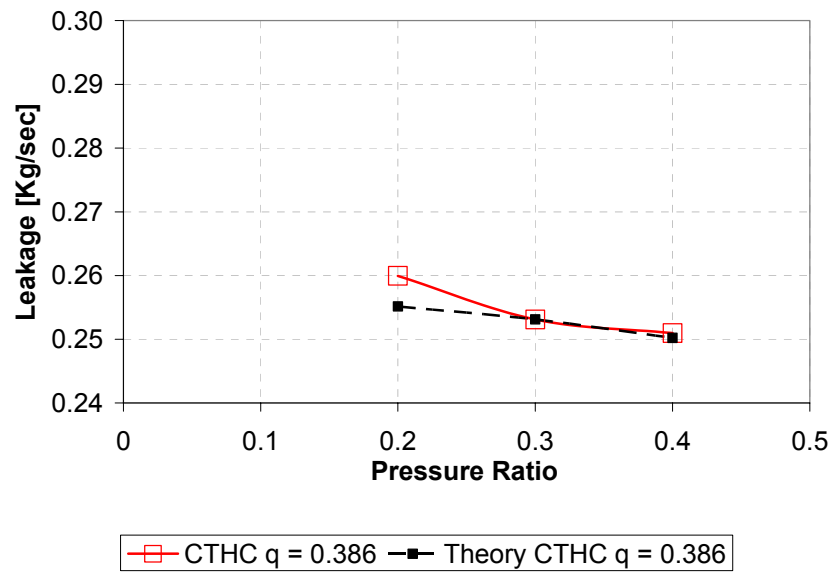


Figure 15 Experimental and Theoretical Leakage for CTHC $q = 0.386$ with Zero Preswirl, $\omega = 20,200$ RPM, and $P_i = 69$ bar (1,000 psi)

SUMMARY AND CONCLUSIONS

This research had the following objectives: (1) test convergent-tapered honeycomb seals and see how the rotordynamic characteristics and leakage compare to predictions by the two-control-volume theory by Kleynhans and Childs, and (2) compare the results from convergent-tapered honeycomb seals to the constant clearance honeycomb seals, which served as a reference in terms of a convergent taper's impact on dynamic and static characteristics. The testing parameters varied to determine the characteristics of the seals were: pressure ratio, radial clearance, and rotor speed. The only supply pressure was 69 bar (1,000 psi).

Results support that constant clearance honeycomb seals (CCHC) produced lower direct stiffness coefficients at all frequencies than convergent-tapered honeycomb seals (CTHC). The cross-coupled stiffness also increased with taper at low frequencies. Conversely, the taper on the seals does not influence significantly the cross-coupled stiffness at higher frequencies.

Results also sustain that the taper on the seals does increase the direct damping coefficients. The magnitude of the coefficients for the cross-coupled damping also increases with taper, especially at lower frequencies.

The taper has the same impact and behavior on effective stiffness with respect to direct stiffness at all frequencies. Consequently, taper does eliminate the possibility of having negative static stiffness when obtained with constant clearance seals. The magnitude of effective damping also increases with taper for all frequencies. Conversely, once it passed the cross-over frequency the magnitude of the effective damping decreases drastically with increasing q . The cross-over frequency increases with both taper and when increasing q .

Results also demonstrated that constant clearance honeycomb seals have less leakage than convergent-tapered honeycomb seals. Data show an increment of approximately 20 percent for CTHC $q = 0.24$ in comparison to CCHC.

The experimental results were compared to theoretical predictions by the two-control-volume theory by Kleynhans and Childs. All rotordynamic coefficients were reasonably predicted for all cases. The model does a better job predicting the cross-coupled stiffness and damping coefficients rather than the direct stiffness and damping

coefficients. Also the two-control-volume model predicts better the dynamic characteristics of CCHC ($q = 0$), and does not predict well the effective stiffness and damping for CTHC $q = 0.386$.

REFERENCES

- [1] Camatti, M., Vannini, G., Fulton, J., and Hopenwasser, F., "Instability of High Pressure Compressor Equipped with Honeycomb Seals," Proceeding of the Thirty-Second Turbomachinery Symposium, Turbomachinery Laboratory, Texas A&M University, College Station, 2003, pp 39-48.
- [2] Dawson, M., 2000, "A Comparison of the Static and Dynamic Characteristics of Straight-Bore and Convergent Tapered-Bore Honeycomb Annular Gas Seals," M.S. Thesis, Texas A&M University, College Station.
- [3] Nelson, C. C., 1984, "Analysis for Leakage and Rotordynamic Coefficients of Surface Roughened Tapered Annular Gas Seals," ASME Journal of Engineering for Gas Turbines and Power," **106**, pp. 927-934.
- [4] Nelson, C. C., 1985, "Rotordynamic Coefficients for Compressible Flow in Tapered Annular Seals," Journal of Tribology, **107**, pp. 318-325.
- [5] Hirs, G. G., 1953, "A Bulk-Flow Theory for Turbulence in Lubricant Films," ASME Journal of Lubrication Technology," **95**, pp. 137-146.
- [6] Childs, D. W., 1983, "Dynamic Analysis of Turbulent Annular Seals Based on Hirs' Lubrication Equations," ASME Journal of Lubrication Technology, **105**, pp. 429-436.
- [7] Childs, D. W., 1983, "Finite-Length Solutions for Rotordynamic Coefficients of Turbulent Annular Seals," ASME Journal of Lubrication Technology, **105**, pp. 437-444.
- [8] Nelson, C. C., Childs, D. W., Nicks, C., Elrod, D., 1986, "Theory versus Experiment for the Rotordynamic Coefficients of Annular Gas Seals: Part 2 – Constant-Clearance and Convergent Tapered Geometry," ASME Journal of Tribology, **108**, pp. 433-438.
- [9] Fleming, D. P., 1979, "Stiffness of Straight and Tapered Annular Gas Path Seals," ASME Journal of Lubrication Technology, **101**, No. 3, pp. 349-355.
- [10] Fleming, D. P., 1980, "Damping in Ring Seals for Compressible Fluids," Rotordynamic Instability Problems of High Performance Turbomachinery, NASA CP No. 2133, Proceedings of a workshop held at Texas A&M University, College Station, pp. 169-188.

- [11] Ha, T., and Childs, D., 1994, "Annular Honeycomb-Stator Turbulent Gas Seal Analysis Using New Friction-Factor Model Based on Flat Plate Tests," ASME Journal of Tribology, **116**, pp. 352-360.
- [12] Kleynhans, G., and Childs, D., 1997, "The Acoustic Influence of Cell Depth on the Rotordynamic Characteristics of Smooth-Rotor/Honeycomb-Stator Annular Gas Seals," ASME Trans., Journal of Engineering for Gas Turbines and Power, October 1997, **119**, No. 4, pp. 949-957.
- [13] Childs, D., Elrod, D., Hale, K., (1989), "Annular Honeycomb Seals: Test Results for Leakage and Rotordynamic Coefficients; Comparison to Labyrinth and Smooth Configurations", ASME Journal of Tribology, **111**, pp. 293-301.
- [14] Weatherwax, M., and Childs, D., 2002, "The Influence of Eccentricity Effects on the Rotordynamic Coefficients of a High-Pressure Honeycomb Annular Gas Seal, Measurements versus Predictions," ASME Paper 2002-TRIB-207.
- [15] Sprowl, T., 2003, "A Study of the Effects of Inlet Preswirl on the Dynamic Coefficients of a Straight-Bore Honeycomb Gas Damper Seal", M.S. Thesis, Turbomachinery Laboratory, Texas A&M University, College Station.
- [16] Wade, J., 2001, "Test Versus Predictions for Rotordynamic Coefficients and Leakage Rates of Hole-Pattern Gas Seals at Two Clearances in Choked and Unchoked Conditions, " M.S. Thesis, Department of Mechanical Engineering, Texas A&M University, College Station.
- [17] Dawson, M., Childs, D., Holt, C., and Phillips, S., 2002, "Theory Versus Experiments for the Dynamic Impedances of Annular Gas Seals: Part 1 – Test Facility and Apparatus," ASME J. Eng. Gas Turbines Power, **24**, pp. 958-963.
- [18] Childs, D., and Hale, K., 1994, "A Test Apparatus and Facility to Identify the Rotordynamic Coefficients of High-Speed Hydrostatic Bearings," ASME Journal of Tribology, **116**, pp. 337-334.
- [19] Seifert, B., 2005, "Measurements versus Predictions for Rotordynamic Coefficients and Leakage Rates for a Novel Hole-Pattern Gas Seal," M.S. Thesis, Texas A&M University, College Station.
- [20] Kurtin, K. A., Childs, D. W., San Andres, L. A., and Hale, R. K., 1993, "Experimental Versus Theoretical Characteristics of a High-Speed Hybrid

(Combination Hydrostatic and Hydrodynamic) Bearing,” ASME Journal of Tribology, **115**, pp. 160-169.

APPENDIX A

Exact test conditions

Table 5 shows exact inlet and exit temperature and pressure, and rotor speed data for all tests.

Table 5 Exact Test Conditions

Pi (bar)	Pe (bar)	Pressure Ratio (%)	ω (RPM)	Ti (K)	Te (K)
$q = 0.24$					
69.88	20.52	29.4	10,200	299.39	296.67
70.09	28.28	40.3		296.92	293.29
70.02	32.66	46.6		300.64	298.93
69.74	20.37	29.2	15,200	299.82	297.78
69.85	27.79	39.8		304.52	300.95
70.13	32.57	46.4		300.69	299.24
69.71	20.21	29.0	20,200	300.19	298.79
69.87	27.75	39.7		300.26	297.50
69.95	32.32	46.2		300.80	299.88
$q = 0.386$					
70.11	15.90	22.7	10,200	287.68	286.05
70.06	20.57	29.4		292.02	289.94
70.30	27.54	39.2		291.68	289.63
70.36	16.09	22.9	15,200	291.17	289.18
70.05	20.27	28.9		292.82	291.40
70.10	27.14	38.7		292.41	291.13
70.17	15.66	22.3	20,200	292.18	291.82
69.83	19.70	28.2		293.59	293.25
70.28	26.43	37.6		291.35	289.66

APPENDIX B

The measured impedances at different conditions are given in the following tables.

Table 6 Zero Preswirl, PR = 30%, 10,200 rpm for $q = 0.24$

f	RZ _{xx}	Iz _{xx}	RZ _{xy}	Iz _{xy}	RZ _{yx}	Iz _{yx}	RZ _{yy}	Iz _{yy}	RZ _{xx}	Iz _{xx}	RZ _{xy}	Iz _{xy}	RZ _{yx}	Iz _{yx}	RZ _{yy}	Iz _{yy}
20	35.42	9.64	-103.42	97.84	103.59	-97.81	35.51	9.58	40.70	24.88	179.46	133.47	179.46	133.47	40.70	24.88
30	169.69	7.61	53.17	69.69	-52.95	-69.73	169.79	7.70	174.28	36.15	36.28	88.80	36.28	88.80	174.28	36.15
40	23.17	3.79	7.06	-5.62	-6.86	5.75	23.44	4.00	4.03	2.22	5.34	5.24	5.35	5.25	4.02	2.20
50	25.22	12.38	10.78	1.27	-10.75	-1.09	25.03	11.62	5.36	6.32	6.45	5.08	6.45	5.08	5.36	6.32
70	26.90	7.34	6.67	-7.50	-6.41	7.52	26.78	7.34	0.47	3.05	2.71	2.13	2.71	2.13	0.48	3.05
80	25.41	6.54	1.82	-2.87	-1.53	2.79	25.27	6.62	2.62	2.05	2.33	6.09	2.33	6.09	2.62	2.05
90	28.03	6.97	0.45	0.87	-0.14	-0.99	27.93	7.14	3.68	3.25	5.39	6.15	5.39	6.15	3.68	3.25
100	27.79	9.78	1.27	-1.23	-0.96	1.08	27.77	9.93	2.91	2.87	6.90	4.60	6.90	4.60	2.91	2.87
110	29.96	11.83	-1.47	-1.99	1.79	1.71	29.98	12.07	2.89	3.76	3.45	5.01	3.45	5.01	2.89	3.76
130	31.22	14.75	2.53	2.11	-2.28	-2.58	31.30	14.99	5.09	4.78	4.87	1.62	4.87	1.62	5.09	4.78
140	28.80	15.53	2.63	-5.98	-2.73	5.32	28.85	15.88	1.00	1.93	3.80	5.19	3.81	5.19	1.00	1.93
150	27.27	13.49	3.70	-4.66	-3.95	4.02	27.45	13.72	2.38	1.32	1.73	3.79	1.73	3.79	2.38	1.31
160	28.39	13.46	8.66	-9.09	-9.31	8.51	28.56	13.83	2.51	2.85	6.66	5.98	6.66	5.98	2.51	2.85
190	31.23	9.89	1.28	-0.13	-2.65	0.63	31.67	10.82	1.22	1.16	3.00	1.17	3.00	1.17	1.22	1.16
200	33.74	10.34	0.97	-2.82	-1.29	3.33	33.99	10.52	3.61	1.83	5.01	3.05	5.01	3.05	3.61	1.83
210	30.37	10.67	2.86	0.85	-3.60	-0.17	30.55	11.16	1.06	1.97	3.25	5.69	3.25	5.69	1.06	1.97
220	32.47	12.55	6.10	-1.89	-6.83	2.94	32.66	12.99	2.86	2.60	5.36	5.68	5.36	5.68	2.86	2.60
230	31.65	10.55	2.76	0.63	-3.37	0.85	31.70	10.90	3.36	1.36	2.12	2.96	2.12	2.96	3.36	1.36
250	35.75	10.13	1.52	1.94	-1.57	0.40	35.48	10.88	6.39	4.21	13.78	14.11	3.89	12.02	16.90	16.72
260	38.04	8.29	5.32	-0.77	-4.62	3.48	37.62	8.33	7.50	8.10	6.14	9.63	6.13	9.63	7.52	8.13
270	32.67	3.83	1.82	-2.91	0.20	4.82	30.49	5.33	4.22	2.79	4.78	3.38	4.78	3.38	4.23	2.80
280	29.78	6.37	4.05	-1.53	-3.53	2.99	29.52	9.24	2.64	4.38	4.55	4.53	4.55	4.53	2.64	4.38
290	31.28	8.63	-0.06	-2.77	0.15	5.02	31.15	11.16	4.37	6.43	4.62	7.35	4.62	7.35	4.37	6.43
310	33.57	10.12	11.80	1.89	-10.38	2.87	34.16	13.28	2.41	8.53	11.05	3.84	11.05	3.84	2.41	8.53
320	32.01	10.49	3.67	0.62	-2.94	4.59	33.20	14.11	3.78	2.37	2.13	3.17	2.13	3.17	3.78	2.37

Table 7 Zero Preswirl, PR = 30%, 15,200 rpm for $q = 0.24$

f	RZ _{xx}	Iz _{xx}	RZ _{xy}	Iz _{xy}	RZ _{yx}	Iz _{yx}	RZ _{yy}	Iz _{yy}	RZ _{xx}	Iz _{xx}	RZ _{xy}	Iz _{xy}	RZ _{yx}	Iz _{yx}	RZ _{yy}	Iz _{yy}
20	31.73	-2.53	-3.65	10.75	3.82	-10.72	31.81	-2.59	22.39	7.89	20.54	18.82	20.54	18.82	22.39	7.89
30	28.47	-5.83	40.56	-1.43	-40.34	1.39	28.57	-5.74	43.49	17.77	37.22	12.58	37.22	12.58	43.49	17.77
40	25.80	4.28	8.76	-5.30	-8.56	5.44	26.07	4.50	2.56	2.61	3.46	2.86	3.47	2.87	2.54	2.59
50	26.99	1.23	9.16	-10.35	-9.14	10.54	26.80	0.47	1.58	1.44	3.10	2.32	3.10	2.32	1.58	1.44
70	25.75	4.40	6.93	-6.55	-6.67	6.57	25.63	4.40	1.67	0.97	5.42	3.75	5.42	3.75	1.67	0.97
80	25.16	6.68	7.82	-6.32	-7.53	6.24	25.02	6.76	2.97	2.20	5.25	2.34	5.25	2.34	2.97	2.20
90	27.32	7.41	8.06	-2.98	-7.75	2.87	27.22	7.57	3.29	3.15	2.52	1.18	2.52	1.18	3.29	3.15
100	28.18	7.78	0.89	-4.81	-0.58	4.66	28.17	7.93	2.99	1.88	4.27	3.56	4.27	3.56	2.99	1.88
110	26.51	9.57	4.78	-3.78	-4.45	3.50	26.54	9.81	4.37	1.49	3.45	4.22	3.45	4.22	4.37	1.49
130	29.79	11.54	5.42	-7.21	-5.17	6.74	29.87	11.78	2.42	3.58	3.28	3.47	3.28	3.47	2.42	3.58
140	28.87	12.34	5.31	-5.58	-5.41	4.91	28.93	12.69	2.38	2.06	2.12	5.86	2.12	5.86	2.38	2.06
150	27.87	11.45	3.12	-3.06	-3.38	2.42	28.05	11.68	1.39	2.25	1.62	3.53	1.62	3.53	1.39	2.25
160	29.16	9.86	3.24	-1.31	-3.88	0.73	29.33	10.23	0.59	1.35	1.18	2.24	1.18	2.24	0.59	1.35
190	29.58	9.97	0.14	-1.45	-1.51	1.95	30.03	10.90	1.25	1.46	1.59	1.40	1.59	1.40	1.25	1.46
200	30.82	9.99	1.62	-1.19	-1.94	1.70	31.07	10.17	2.36	0.50	1.44	3.59	1.44	3.59	2.36	0.50
210	31.74	10.19	1.96	-1.53	-2.70	2.22	31.92	10.67	1.54	0.85	1.99	1.71	1.99	1.72	1.54	0.85
220	32.57	10.28	4.39	1.33	-5.11	-0.27	32.75	10.72	0.34	1.61	2.04	2.80	2.04	2.80	0.34	1.62
230	32.60	11.89	-3.02	4.00	2.41	-2.52	32.65	12.24	1.24	2.43	1.58	2.77	1.58	2.77	1.24	2.43
250	22.34	10.82	-10.23	-26.84	10.18	29.19	22.07	11.57	6.10	4.22	13.79	9.74	3.96	6.34	16.79	16.72
260	17.44	11.44	-11.57	-23.65	12.27	26.36	17.01	11.49	3.31	1.96	2.76	2.59	2.74	2.57	3.37	2.06
270	36.06	49.61	-25.57	14.76	27.60	-12.85	33.88	51.10	12.30	7.89	5.04	9.52	5.04	9.52	12.30	7.89
280	49.84	20.55	-7.83	11.74	8.35	-10.28	49.58	23.42	4.40	8.94	8.80	3.80	8.80	3.80	4.40	8.94
290	42.05	10.00	-5.77	5.11	5.86	-2.86	41.92	12.53	3.76	3.37	5.52	6.76	5.52	6.76	3.76	3.37
310	34.59	7.75	7.02	2.60	-5.59	2.15	35.19	10.91	3.26	6.05	7.95	2.32	7.95	2.32	3.26	6.05
320	35.25	8.33	-1.62	-1.47	2.36	6.68	36.45	11.95	2.34	2.75	3.15	6.84	3.15	6.84	2.34	2.75

Table 8 Zero Preswirl, PR = 30%, 20,200 rpm for $q = 0.24$

f	RZ _{xx}	Iz _{xx}	RZ _{xy}	Iz _{xy}	RZ _{yx}	Iz _{yx}	RZ _{yy}	Iz _{yy}	RZ _{xx}	Iz _{xx}	RZ _{xy}	Iz _{xy}	RZ _{yx}	Iz _{yx}	RZ _{yy}	Iz _{yy}
20	29.64	5.89	9.62	-11.61	-9.44	11.64	29.72	5.83	4.69	5.62	10.78	5.29	10.78	5.29	4.69	5.62
30	24.30	7.71	32.75	42.13	-32.53	-42.17	24.40	7.80	21.12	17.40	42.81	33.10	42.81	33.10	21.12	17.40
40	23.09	2.13	11.47	-7.24	-11.26	7.38	23.36	2.34	1.63	2.71	1.22	2.63	1.24	2.65	1.59	2.69
50	26.20	2.21	10.59	-8.70	-10.57	8.89	26.01	1.46	3.02	1.80	2.99	3.79	2.99	3.79	3.02	1.79
70	24.82	3.00	8.83	-3.87	-8.57	3.90	24.70	2.99	1.05	0.72	3.09	3.24	3.09	3.24	1.05	0.72
80	25.41	6.24	8.08	-5.67	-7.79	5.59	25.27	6.32	1.29	1.84	2.13	2.37	2.13	2.37	1.29	1.84
90	27.15	4.82	5.47	-5.91	-5.16	5.80	27.05	4.98	2.39	2.43	2.09	1.58	2.09	1.58	2.39	2.43
100	25.62	8.14	7.18	-4.75	-6.86	4.60	25.60	8.29	0.38	1.59	2.32	1.50	2.32	1.50	0.38	1.59
110	26.60	9.33	7.70	-4.42	-7.37	4.13	26.63	9.57	1.21	1.36	2.16	0.82	2.16	0.82	1.21	1.36
130	26.49	8.28	5.10	-5.79	-4.85	5.32	26.57	8.52	1.04	1.57	1.87	2.74	1.87	2.74	1.04	1.57
140	29.35	9.37	6.10	-5.90	-6.20	5.24	29.40	9.72	1.82	1.50	0.63	2.17	0.63	2.17	1.81	1.51
150	28.18	9.36	4.45	-3.85	-4.70	3.21	28.37	9.59	0.86	1.10	2.58	2.39	2.58	2.39	0.86	1.10
160	28.54	8.38	4.79	-4.31	-5.44	3.73	28.71	8.74	1.07	1.30	1.87	2.61	1.87	2.61	1.07	1.30
190	30.43	9.40	2.00	-3.24	-3.37	3.74	30.88	10.33	0.84	0.58	1.54	2.15	1.54	2.14	0.83	0.58
200	31.11	10.86	2.57	-2.52	-2.89	3.03	31.36	11.04	1.45	0.81	0.96	2.42	0.96	2.42	1.45	0.81
210	32.06	9.16	2.19	-2.55	-2.93	3.23	32.24	9.64	0.80	0.81	0.93	1.30	0.93	1.30	0.80	0.81
220	32.94	10.19	3.78	-2.79	-4.50	3.84	33.12	10.63	1.24	2.09	2.65	2.28	2.65	2.28	1.24	2.09
230	33.25	9.34	4.97	-1.01	-5.58	2.50	33.30	9.69	1.12	1.07	1.46	1.52	1.46	1.52	1.12	1.07
250	34.54	8.99	3.85	-2.11	-3.90	4.45	34.27	9.74	2.78	4.15	13.76	8.76	3.82	4.69	15.89	16.70
260	36.50	8.72	4.96	-4.05	-4.26	6.76	36.07	8.76	1.97	3.16	2.06	1.75	2.04	1.72	2.07	3.22
270	37.91	4.71	5.42	-3.55	-3.39	5.46	35.73	6.20	3.83	2.81	4.34	2.98	4.34	2.98	3.84	2.81
280	34.98	6.35	5.16	-2.13	-4.64	3.58	34.72	9.22	1.54	1.28	2.66	0.76	2.66	0.76	1.54	1.28
290	37.66	7.28	3.10	-2.53	-3.01	4.79	37.53	9.81	2.99	2.76	4.20	3.40	4.20	3.40	2.99	2.76
310	41.53	9.18	0.60	4.01	0.83	0.75	42.13	12.34	2.78	2.98	6.19	2.88	6.19	2.88	2.78	2.98
320	45.12	9.26	-4.09	8.59	4.82	-3.38	46.32	12.88	3.67	4.72	5.74	8.29	5.74	8.29	3.67	4.72

Table 9 Zero Preswirl, PR = 40%, 10,200 rpm for $q = 0.24$

f	RZ _{xx}	Iz _{xx}	RZ _{xy}	Iz _{xy}	RZ _{yx}	Iz _{yx}	RZ _{yy}	Iz _{yy}	RZ _{xx}	Iz _{xx}	RZ _{xy}	Iz _{xy}	RZ _{yx}	Iz _{yx}	RZ _{yy}	Iz _{yy}
20	26.03	10.75	14.63	-11.46	-14.46	11.49	26.12	10.69	12.36	7.04	18.83	6.30	18.83	6.30	12.36	7.04
30	27.05	-0.58	12.79	-2.87	-12.57	2.83	27.15	-0.49	19.11	21.60	7.55	4.27	7.55	4.27	19.11	21.60
40	23.02	0.60	6.82	-3.08	-6.62	3.22	23.29	0.81	1.92	2.48	1.42	2.42	1.44	2.44	1.89	2.46
50	21.31	8.94	6.18	-3.64	-6.16	3.83	21.12	8.18	3.04	4.20	1.28	2.04	1.28	2.04	3.04	4.20
70	23.68	5.01	6.39	-2.07	-6.13	2.09	23.56	5.00	2.61	2.53	2.10	1.26	2.10	1.26	2.61	2.53
80	23.83	8.01	5.30	-2.34	-5.01	2.26	23.69	8.09	1.73	1.44	2.44	1.04	2.44	1.04	1.73	1.44
90	26.19	11.13	5.27	-2.96	-4.96	2.85	26.08	11.30	2.90	4.83	2.91	2.44	2.91	2.44	2.90	4.83
100	23.14	10.35	5.86	-1.89	-5.55	1.74	23.12	10.50	1.75	2.86	2.47	1.14	2.47	1.14	1.75	2.86
110	25.10	11.84	4.56	-3.64	-4.23	3.35	25.13	12.08	1.48	3.28	1.50	2.45	1.50	2.45	1.48	3.28
130	27.09	15.09	5.07	-2.06	-4.82	1.59	27.17	15.32	2.57	4.92	2.17	1.50	2.17	1.50	2.57	4.92
140	27.78	13.36	3.67	-2.30	-3.76	1.64	27.83	13.71	4.35	3.81	2.15	2.15	2.15	2.15	4.35	3.81
150	29.32	13.29	2.74	-3.83	-2.99	3.19	29.51	13.52	1.74	2.71	1.10	2.65	1.10	2.65	1.74	2.70
160	29.63	13.89	2.73	-3.02	-3.37	2.44	29.80	14.25	2.26	1.58	1.33	0.89	1.33	0.89	2.26	1.58
190	34.16	12.75	2.05	-2.45	-3.42	2.95	34.60	13.68	3.38	4.12	1.79	0.83	1.79	0.83	3.38	4.12
200	33.53	12.45	1.92	-0.70	-2.24	1.21	33.78	12.63	2.43	1.02	1.47	1.46	1.47	1.46	2.43	1.02
210	36.01	14.39	2.75	-3.37	-3.49	4.05	36.19	14.88	5.34	3.32	1.10	3.03	1.11	3.03	5.34	3.32
220	35.19	12.23	2.84	0.03	-3.56	1.03	35.37	12.67	4.16	2.41	1.90	1.05	1.90	1.05	4.16	2.41
230	38.28	15.44	1.19	0.35	-1.80	1.14	38.34	15.78	5.52	4.74	2.05	1.45	2.05	1.45	5.52	4.74
250	39.01	11.96	5.37	-4.70	-5.43	7.04	38.74	12.71	6.83	3.56	13.61	8.56	3.25	4.32	17.07	16.56
260	39.19	10.51	2.72	-2.87	-2.01	5.58	38.76	10.56	4.22	9.04	2.64	5.23	2.63	5.23	4.26	9.06
270	35.89	7.47	4.91	-1.95	-2.89	3.86	33.71	8.96	13.64	5.80	2.71	0.49	2.72	0.48	13.64	5.81
280	43.24	7.04	4.69	-3.52	-4.17	4.98	42.98	9.91	10.81	7.29	4.71	3.78	4.71	3.78	10.81	7.29
290	44.71	10.21	3.47	-7.11	-3.38	9.37	44.57	12.74	8.56	7.95	4.22	4.83	4.22	4.83	8.56	7.95
310	34.16	5.90	-4.74	3.01	6.17	1.75	34.76	9.06	9.82	10.28	4.35	5.13	4.35	5.13	9.82	10.28
320	34.85	2.49	-5.52	3.91	6.25	1.30	36.05	6.10	6.02	5.98	3.07	4.08	3.07	4.08	6.02	5.98

Table 10 Zero Preswirl, PR = 40%, 15,200 rpm for $q = 0.24$

f	RZ _{xx}	Iz _{xx}	RZ _{xy}	Iz _{xy}	RZ _{yx}	Iz _{yx}	RZ _{yy}	Iz _{yy}	RZ _{xx}	Iz _{xx}	RZ _{xy}	Iz _{xy}	RZ _{yx}	Iz _{yx}	RZ _{yy}	Iz _{yy}
20	22.58	12.52	11.20	-6.26	-11.03	6.29	22.67	12.46	6.09	5.16	4.66	9.22	4.66	9.22	6.09	5.16
30	26.02	20.01	9.82	0.52	-9.60	-0.56	26.12	20.10	12.34	14.80	5.91	3.63	5.91	3.64	12.34	14.80
40	21.68	4.13	8.39	-2.94	-8.19	3.08	21.95	4.34	0.95	1.47	0.96	0.98	1.00	1.01	0.89	1.44
50	23.45	8.15	7.20	-4.78	-7.18	4.97	23.26	7.39	1.33	2.21	1.88	1.06	1.88	1.06	1.33	2.21
70	23.62	3.18	6.53	-4.01	-6.27	4.03	23.50	3.18	0.74	1.52	0.85	1.12	0.85	1.12	0.75	1.52
80	22.91	6.67	5.91	-4.48	-5.62	4.40	22.77	6.74	0.67	2.11	1.22	0.49	1.22	0.48	0.68	2.11
90	24.31	5.99	4.10	-3.48	-3.79	3.37	24.20	6.15	0.81	1.28	1.91	2.78	1.91	2.78	0.81	1.28
100	24.14	9.77	6.31	-2.94	-6.00	2.79	24.12	9.92	1.44	0.72	1.87	1.09	1.87	1.09	1.44	0.72
110	24.51	10.39	4.08	-3.36	-3.76	3.07	24.54	10.62	1.56	0.66	1.12	0.52	1.12	0.52	1.56	0.66
130	25.14	7.58	4.84	-3.97	-4.58	3.51	25.22	7.82	1.33	0.93	1.62	0.18	1.62	0.18	1.33	0.93
140	28.18	13.04	5.06	-3.94	-5.15	3.28	28.24	13.39	1.93	1.35	1.61	0.81	1.61	0.81	1.93	1.35
150	28.63	9.74	4.61	-4.86	-4.86	4.22	28.81	9.97	0.97	0.68	1.36	0.80	1.36	0.80	0.97	0.68
160	30.42	10.07	4.02	-4.07	-4.66	3.49	30.59	10.44	2.42	0.58	1.50	0.85	1.50	0.85	2.42	0.58
190	29.01	9.15	2.59	-2.08	-3.96	2.58	29.45	10.08	0.93	1.14	1.05	0.77	1.05	0.77	0.93	1.14
200	29.30	8.84	3.40	-1.80	-3.72	2.31	29.55	9.02	1.47	2.94	0.49	1.33	0.49	1.33	1.47	2.94
210	30.97	14.13	3.45	-2.69	-4.19	3.37	31.16	14.62	1.46	1.38	1.63	1.55	1.63	1.55	1.46	1.38
220	31.58	8.72	2.81	0.52	-3.54	0.54	31.77	9.16	1.40	3.34	2.11	2.55	2.11	2.55	1.40	3.34
230	35.68	13.03	1.12	1.63	-1.73	-0.15	35.73	13.38	3.71	1.33	2.23	1.41	2.23	1.41	3.71	1.33
250	19.96	12.86	-14.16	-30.75	14.11	33.10	19.69	13.61	3.64	2.79	13.75	10.40	3.80	7.31	16.06	16.41
260	12.93	9.63	-32.64	-26.36	33.34	29.07	12.51	9.68	2.19	2.87	7.44	3.39	7.43	3.37	2.28	2.94
270	40.58	15.24	6.28	9.40	-4.26	-7.49	38.40	16.73	7.08	4.39	7.57	4.22	7.57	4.22	7.08	4.39
280	39.10	15.78	5.43	0.06	-4.91	1.40	38.84	18.66	2.67	8.52	5.35	2.03	5.35	2.03	2.67	8.52
290	36.29	19.43	7.56	-6.70	-7.47	8.96	36.16	21.96	1.70	3.41	2.91	4.03	2.91	4.03	1.70	3.41
310	37.41	0.47	-6.01	-1.41	7.44	6.16	38.00	3.64	5.63	8.16	0.94	1.82	0.94	1.81	5.63	8.16
320	47.53	1.92	-5.27	1.76	6.01	3.45	48.73	5.54	1.92	1.79	2.26	1.47	2.26	1.47	1.92	1.78

Table 11 Zero Preswirl, PR = 40%, 20,200 rpm for $q = 0.24$

f	RZ _{xx}	Iz _{xx}	RZ _{xy}	Iz _{xy}	RZ _{yx}	Iz _{yx}	RZ _{yy}	Iz _{yy}	RZ _{xx}	Iz _{xx}	RZ _{xy}	Iz _{xy}	RZ _{yx}	Iz _{yx}	RZ _{yy}	Iz _{yy}
20	19.80	4.75	20.17	6.16	-20.00	-6.13	19.89	4.69	2.62	4.26	7.52	9.86	7.52	9.86	2.62	4.26
30	27.28	-7.66	12.97	-0.15	-12.75	0.11	27.38	-7.57	7.25	7.18	17.68	16.93	17.68	16.93	7.25	7.18
40	22.47	3.65	11.87	-5.51	-11.67	5.64	22.74	3.86	0.92	0.82	0.40	1.08	0.48	1.11	0.85	0.76
50	22.81	8.37	11.24	-5.22	-11.22	5.41	22.62	7.61	1.50	3.55	2.02	1.24	2.02	1.24	1.50	3.55
70	24.86	5.95	9.29	-6.81	-9.03	6.84	24.74	5.95	1.64	1.40	1.11	1.82	1.11	1.82	1.64	1.40
80	23.06	5.09	6.84	-5.54	-6.55	5.46	22.92	5.17	1.09	2.41	1.70	0.78	1.70	0.78	1.09	2.41
90	24.38	7.43	8.33	-4.26	-8.02	4.15	24.28	7.59	1.11	1.06	1.12	1.70	1.12	1.70	1.11	1.06
100	23.68	9.28	6.56	-4.78	-6.24	4.63	23.66	9.43	1.49	1.22	1.31	1.70	1.31	1.70	1.49	1.22
110	22.82	9.16	6.11	-3.81	-5.78	3.52	22.85	9.39	1.43	1.62	0.86	0.85	0.86	0.85	1.43	1.62
130	26.08	12.26	5.61	-4.52	-5.36	4.05	26.15	12.50	0.78	1.69	0.63	0.84	0.63	0.84	0.78	1.69
140	27.27	12.64	5.50	-5.76	-5.60	5.09	27.33	12.99	0.93	1.34	0.35	1.53	0.35	1.53	0.93	1.34
150	27.11	12.26	5.03	-4.90	-5.29	4.26	27.29	12.50	0.78	0.35	1.22	1.34	1.22	1.34	0.78	0.34
160	28.56	13.00	4.14	-4.78	-4.79	4.21	28.73	13.37	1.20	1.00	1.15	0.54	1.15	0.54	1.20	1.00
190	29.00	12.72	3.46	-3.66	-4.83	4.16	29.44	13.66	0.87	0.66	0.52	0.87	0.52	0.87	0.87	0.66
200	32.28	13.85	3.94	-4.18	-4.26	4.69	32.53	14.03	1.71	1.05	0.58	0.83	0.58	0.83	1.71	1.05
210	31.46	13.13	2.86	-4.35	-3.60	5.04	31.65	13.62	0.77	0.70	0.69	0.82	0.69	0.82	0.77	0.70
220	32.99	13.83	2.14	-3.25	-2.87	4.31	33.18	14.27	1.32	1.41	1.19	1.59	1.19	1.59	1.32	1.41
230	32.74	13.47	3.39	-2.66	-3.99	4.14	32.79	13.81	1.19	1.27	1.38	0.69	1.38	0.69	1.19	1.27
250	40.58	8.38	6.20	-2.24	-4.17	4.15	38.40	9.87	3.53	2.95	13.60	8.48	3.23	4.16	16.04	16.44
260	40.58	8.38	6.20	-2.24	-4.17	4.15	38.40	9.87	2.57	1.69	1.57	1.66	1.55	1.63	2.64	1.80
270	40.58	8.38	6.20	-2.24	-4.17	4.15	38.40	9.87	2.47	1.52	1.86	1.40	1.87	1.40	2.47	1.53
280	33.47	11.25	6.48	-2.06	-5.96	3.51	33.21	14.12	3.17	4.22	1.41	2.58	1.41	2.58	3.17	4.22
290	35.61	13.75	9.06	-4.83	-8.97	7.09	35.47	16.28	1.76	3.21	3.01	1.81	3.01	1.81	1.76	3.22
310	39.72	12.45	-9.16	-1.98	10.59	6.74	40.31	15.62	5.44	4.90	0.61	3.37	0.62	3.36	5.44	4.90
320	51.37	17.97	-18.27	-1.54	19.00	6.75	52.57	21.58	2.98	1.75	3.06	1.43	3.06	1.44	2.98	1.74

Table 12 Zero Preswirl, PR = 46%, 10,200 rpm for $q = 0.24$

f	RZ _{xx}	Iz _{xx}	RZ _{xy}	Iz _{xy}	RZ _{yx}	Iz _{yx}	RZ _{yy}	Iz _{yy}	RZ _{xx}	Iz _{xx}	RZ _{xy}	Iz _{xy}	RZ _{yx}	Iz _{yx}	RZ _{yy}	Iz _{yy}
20	22.86	6.08	10.46	-10.58	-10.29	10.61	22.94	6.02	2.65	6.19	10.04	10.42	10.04	10.42	2.65	6.19
30	24.99	13.07	22.35	-1.69	-22.13	1.65	25.08	13.16	12.37	5.11	15.54	18.82	15.54	18.82	12.37	5.11
40	20.64	4.61	6.32	-2.44	-6.12	2.57	20.91	4.82	1.45	1.64	1.14	0.53	1.17	0.59	1.40	1.61
50	21.34	5.81	5.95	-2.92	-5.93	3.10	21.15	5.05	2.05	0.75	1.35	1.23	1.35	1.24	2.05	0.75
70	21.71	7.71	4.83	-2.89	-4.57	2.91	21.59	7.70	0.99	0.88	1.34	0.83	1.34	0.83	0.99	0.88
80	21.85	8.03	6.33	-2.57	-6.04	2.49	21.71	8.11	0.96	1.26	1.55	0.49	1.55	0.49	0.96	1.26
90	22.93	10.35	2.60	-4.00	-2.29	3.88	22.83	10.51	1.46	1.68	3.07	1.82	3.07	1.82	1.46	1.68
100	23.29	9.92	1.59	-1.39	-1.28	1.24	23.27	10.07	1.72	1.80	0.77	2.91	0.77	2.91	1.72	1.80
110	23.70	12.91	5.68	-1.35	-5.35	1.06	23.73	13.15	1.20	1.03	1.30	0.76	1.30	0.76	1.20	1.03
130	24.13	12.60	2.12	-2.64	-1.87	2.18	24.21	12.84	1.18	1.86	2.05	1.76	2.05	1.76	1.18	1.86
140	25.87	14.69	3.54	-2.42	-3.63	1.75	25.93	15.04	1.14	1.24	1.02	1.27	1.02	1.27	1.14	1.24
150	26.18	13.20	1.74	-3.14	-1.99	2.50	26.37	13.43	0.89	0.77	2.62	2.05	2.62	2.05	0.89	0.77
160	27.45	14.85	3.23	-4.65	-3.88	4.08	27.62	15.21	1.32	1.09	3.32	1.08	3.32	1.08	1.32	1.09
190	29.62	13.24	0.17	-0.32	-1.54	0.82	30.06	14.17	1.11	0.38	1.47	1.26	1.47	1.26	1.11	0.38
200	29.64	13.65	2.47	-1.32	-2.79	1.83	29.90	13.83	0.56	0.11	1.20	1.34	1.20	1.34	0.56	0.10
210	30.95	14.81	2.21	-1.86	-2.95	2.55	31.14	15.30	0.72	0.49	1.77	0.60	1.77	0.60	0.72	0.49
220	31.61	14.21	2.04	-0.21	-2.76	1.26	31.79	14.65	1.10	0.54	2.32	2.15	2.32	2.15	1.10	0.54
230	31.02	16.92	1.35	1.37	-1.95	0.12	31.07	17.26	1.50	1.65	2.91	1.09	2.91	1.09	1.50	1.65
250	34.63	15.12	2.65	1.57	-2.70	0.77	34.37	15.87	2.73	2.85	13.62	8.84	3.30	4.85	15.88	16.43
260	35.58	17.56	2.04	0.08	-1.33	2.63	35.15	17.61	3.54	3.29	1.52	2.58	1.50	2.56	3.59	3.35
270	36.50	11.05	3.59	-0.51	-1.57	2.42	34.31	12.54	4.00	1.22	2.66	2.21	2.66	2.20	4.00	1.23
280	34.94	13.12	5.42	-1.57	-4.90	3.03	34.68	15.99	4.22	1.74	2.78	1.58	2.79	1.58	4.22	1.74
290	31.07	17.69	7.28	-6.11	-7.19	8.37	30.94	20.22	3.12	2.61	4.69	4.04	4.69	4.04	3.12	2.61
310	42.90	8.04	-3.78	-4.70	5.21	9.45	43.50	11.20	1.55	5.89	1.91	2.07	1.91	2.07	1.55	5.89
320	41.19	10.06	-5.29	-1.72	6.02	6.93	42.39	13.68	1.52	2.65	4.57	3.99	4.57	3.99	1.52	2.65

Table 13 Zero Preswirl, PR = 46%, 15,200 rpm for $q = 0.24$

f	RZ _{xx}	Iz _{xx}	RZ _{xy}	Iz _{xy}	RZ _{yx}	Iz _{yx}	RZ _{yy}	Iz _{yy}	RZ _{xx}	Iz _{xx}	RZ _{xy}	Iz _{xy}	RZ _{yx}	Iz _{yx}	RZ _{yy}	Iz _{yy}
20	19.56	2.23	15.11	0.48	-14.94	-0.45	19.64	2.17	2.18	2.83	7.57	2.97	7.57	2.97	2.18	2.83
30	20.04	3.40	10.65	3.31	-10.43	-3.34	20.14	3.49	5.59	9.90	4.46	7.55	4.46	7.55	5.59	9.90
40	20.38	4.27	8.44	-3.76	-8.23	3.90	20.65	4.48	0.99	0.90	0.74	1.03	0.78	1.06	0.93	0.84
50	20.41	7.38	8.36	-4.82	-8.34	5.01	20.22	6.62	1.07	1.54	1.19	1.70	1.18	1.70	1.07	1.54
70	21.33	7.11	7.06	-4.35	-6.80	4.37	21.21	7.10	0.59	0.95	1.40	1.22	1.40	1.22	0.59	0.95
80	21.73	8.30	5.86	-4.13	-5.57	4.05	21.59	8.38	1.12	0.84	1.10	1.03	1.10	1.03	1.12	0.84
90	22.79	10.66	6.63	-5.02	-6.32	4.91	22.69	10.82	0.53	1.02	1.15	0.79	1.15	0.79	0.53	1.02
100	23.00	10.75	5.77	-3.84	-5.45	3.69	22.98	10.90	2.19	1.00	1.38	0.91	1.38	0.91	2.19	1.00
110	24.58	10.75	4.59	-3.81	-4.27	3.52	24.61	10.98	0.88	0.75	1.27	0.89	1.27	0.89	0.88	0.75
130	24.38	13.25	5.63	-3.26	-5.38	2.79	24.46	13.49	0.91	1.87	0.76	1.03	0.76	1.03	0.91	1.87
140	26.31	11.62	3.18	-5.13	-3.27	4.46	26.36	11.97	0.62	1.75	0.34	1.11	0.34	1.11	0.62	1.75
150	25.86	13.88	3.06	-3.25	-3.32	2.61	26.05	14.11	1.23	0.68	1.69	1.06	1.69	1.06	1.23	0.68
160	26.71	14.49	4.87	-3.95	-5.52	3.37	26.88	14.85	1.17	0.68	1.29	1.12	1.29	1.12	1.17	0.68
190	29.49	14.10	2.24	-2.30	-3.61	2.80	29.93	15.03	0.65	0.97	1.40	0.83	1.40	0.82	0.64	0.98
200	29.82	16.43	3.87	-0.29	-4.19	0.80	30.08	16.61	0.57	1.25	1.16	1.05	1.16	1.05	0.57	1.25
210	31.42	14.76	2.04	-2.60	-2.78	3.28	31.60	15.25	0.38	0.57	0.82	0.73	0.82	0.73	0.38	0.57
220	31.51	15.10	2.81	1.70	-3.53	-0.65	31.69	15.54	1.02	1.15	0.88	1.25	0.88	1.25	1.02	1.16
230	33.75	20.15	-2.08	6.97	1.47	-5.49	33.81	20.50	1.86	1.76	1.62	2.36	1.62	2.36	1.86	1.76
250	27.65	10.40	-6.80	-34.82	6.75	37.17	27.38	11.15	2.58	3.06	13.65	8.41	3.41	4.01	15.85	16.46
260	25.70	4.57	-15.76	-35.59	16.47	38.30	25.27	4.62	2.03	0.90	1.18	2.24	1.15	2.22	2.13	1.09
270	-27.82	53.65	-80.92	-31.20	82.94	33.11	-30.00	55.14	31.81	15.66	17.63	33.02	17.63	33.02	31.81	15.67
280	46.86	11.87	5.81	18.64	-5.29	-17.18	46.60	14.75	2.97	2.77	8.12	4.58	8.12	4.58	2.97	2.77
290	39.74	16.58	6.64	2.76	-6.55	-0.50	39.61	19.11	2.68	3.36	3.17	2.10	3.17	2.10	2.68	3.36
310	44.01	10.80	-4.26	-1.77	5.69	6.52	44.61	13.96	3.31	1.43	2.19	1.81	2.19	1.81	3.31	1.43
320	43.19	11.73	-4.52	-0.03	5.26	5.24	44.38	15.34	3.05	1.93	2.56	2.31	2.56	2.31	3.05	1.93

Table 14 Zero Preswirl, PR = 46%, 20,200 rpm for $q = 0.24$

f	RZ _{xx}	Iz _{xx}	RZ _{xy}	Iz _{xy}	RZ _{yx}	Iz _{yx}	RZ _{yy}	Iz _{yy}	RZ _{xx}	Iz _{xx}	RZ _{xy}	Iz _{xy}	RZ _{yx}	Iz _{yx}	RZ _{yy}	Iz _{yy}
20	19.47	2.95	5.07	0.26	-4.90	-0.23	19.56	2.89	3.31	1.50	7.73	7.10	7.73	7.10	3.31	1.50
30	19.45	2.64	24.00	-6.13	-23.78	6.09	19.55	2.73	6.23	11.72	16.92	11.83	16.92	11.83	6.23	11.72
40	17.64	4.35	11.50	-4.23	-11.30	4.36	17.91	4.56	1.49	1.44	1.76	0.70	1.78	0.74	1.45	1.41
50	20.00	7.42	11.39	-5.71	-11.37	5.89	19.81	6.66	1.55	1.02	1.12	1.99	1.12	1.99	1.55	1.01
70	21.42	7.03	10.10	-4.00	-9.84	4.03	21.30	7.03	1.59	1.48	1.33	1.32	1.33	1.32	1.59	1.48
80	21.36	8.09	7.78	-4.84	-7.48	4.76	21.22	8.17	0.72	1.66	2.07	1.86	2.07	1.86	0.72	1.66
90	21.59	9.67	6.64	-2.76	-6.32	2.65	21.48	9.84	2.32	1.30	1.24	1.16	1.24	1.16	2.32	1.30
100	22.84	10.67	7.23	-4.51	-6.92	4.36	22.82	10.83	0.82	1.25	1.36	2.48	1.36	2.48	0.82	1.25
110	23.90	10.06	6.10	-5.35	-5.77	5.06	23.93	10.30	2.55	2.00	1.96	2.38	1.96	2.38	2.55	2.00
130	25.31	13.82	6.35	-5.32	-6.10	4.86	25.39	14.06	1.72	1.25	1.62	2.61	1.62	2.61	1.72	1.25
140	24.31	13.71	5.43	-3.95	-5.53	3.28	24.36	14.06	1.07	0.89	1.19	1.00	1.19	1.00	1.07	0.89
150	26.19	14.11	3.88	-5.59	-4.13	4.95	26.38	14.34	1.39	0.91	1.19	1.34	1.19	1.34	1.39	0.91
160	27.69	14.20	5.20	-6.91	-5.84	6.33	27.86	14.57	0.90	0.75	1.20	1.98	1.20	1.98	0.90	0.75
190	28.82	13.87	3.88	-3.54	-5.26	4.04	29.26	14.80	0.40	0.86	2.12	0.98	2.12	0.97	0.40	0.86
200	30.97	15.00	4.17	-2.74	-4.49	3.25	31.22	15.18	0.85	1.14	3.46	0.84	3.46	0.84	0.85	1.14
210	29.92	14.62	1.89	-2.95	-2.63	3.63	30.10	15.11	0.98	0.87	1.38	0.83	1.38	0.83	0.98	0.87
220	31.12	15.36	3.34	-3.07	-4.06	4.13	31.31	15.80	1.73	1.77	2.98	1.14	2.98	1.14	1.73	1.77
230	32.16	15.16	2.06	-3.86	-2.67	5.35	32.21	15.51	1.84	1.14	1.61	2.07	1.61	2.07	1.84	1.14
250	34.15	16.23	4.44	-2.45	-4.50	4.80	33.88	16.98	3.34	2.87	13.58	8.82	3.14	4.81	16.00	16.43
260	39.64	17.11	6.57	-2.00	-5.86	4.71	39.21	17.15	4.25	2.76	1.92	1.23	1.89	1.20	4.30	2.83
270	38.81	12.41	6.28	-1.79	-4.25	3.70	36.63	13.90	2.30	4.36	1.88	2.01	1.88	2.00	2.30	4.36
280	34.72	13.30	4.26	-5.49	-3.74	6.95	34.46	16.17	3.39	2.77	5.99	1.71	5.99	1.71	3.39	2.77
290	33.90	17.03	10.66	-7.06	-10.57	9.32	33.77	19.56	3.08	3.32	2.90	3.79	2.90	3.79	3.08	3.32
310	45.17	14.95	-10.74	-2.85	12.17	7.61	45.76	18.11	2.77	3.49	2.21	4.50	2.21	4.50	2.77	3.49
320	52.73	23.85	-21.31	-1.27	22.04	6.47	53.93	27.47	4.63	5.12	7.20	5.70	7.20	5.70	4.63	5.12

Table 15 Zero Preswirl, PR = 20%, 10,200 rpm for $q = 0.386$

f	RZ _{xx}	Iz _{xx}	RZ _{xy}	Iz _{xy}	RZ _{yx}	Iz _{yx}	RZ _{yy}	Iz _{yy}	RZ _{xx}	Iz _{xx}	RZ _{xy}	Iz _{xy}	RZ _{yx}	Iz _{yx}	RZ _{yy}	Iz _{yy}
20	39.16	0.21	21.33	-5.91	-21.15	5.95	39.25	0.15	4.63	6.92	5.06	4.23	5.06	4.23	4.63	6.92
30	40.53	-2.19	-3.15	-19.90	3.37	19.86	40.63	-2.10	4.05	2.86	23.00	22.06	23.00	22.06	4.05	2.86
40	35.95	-1.03	14.72	-8.47	-14.52	8.60	36.22	-0.82	2.63	3.25	2.43	2.76	2.44	2.77	2.60	3.24
50	34.24	-1.14	11.75	-9.23	-11.73	9.42	34.05	-1.89	9.76	11.62	5.09	4.37	5.09	4.37	9.76	11.62
70	35.28	0.04	8.95	-8.39	-8.69	8.41	35.16	0.03	1.89	2.22	1.47	2.06	1.47	2.06	1.89	2.22
80	35.27	1.29	9.17	-5.21	-8.88	5.13	35.13	1.37	1.26	2.49	2.56	4.80	2.56	4.80	1.26	2.49
90	33.02	3.27	7.77	-8.12	-7.46	8.01	32.91	3.44	1.96	1.44	1.29	1.27	1.29	1.27	1.96	1.44
100	33.95	2.85	6.79	-7.36	-6.47	7.21	33.94	3.00	2.77	2.62	1.55	1.32	1.55	1.32	2.77	2.62
110	35.23	4.40	6.97	-7.20	-6.64	6.91	35.25	4.63	1.76	2.57	1.44	1.39	1.44	1.39	1.76	2.58
130	35.96	4.69	4.76	-7.73	-4.51	7.26	36.04	4.93	0.99	0.87	1.93	1.31	1.93	1.31	0.99	0.88
140	37.00	4.43	4.72	-6.94	-4.82	6.27	37.06	4.78	1.56	1.22	0.50	0.94	0.50	0.94	1.56	1.22
150	37.38	5.51	4.52	-7.01	-4.77	6.37	37.57	5.74	0.83	1.32	0.91	0.74	0.91	0.74	0.83	1.32
160	37.23	5.11	4.01	-6.82	-4.65	6.25	37.40	5.48	0.44	0.60	0.65	0.61	0.65	0.61	0.44	0.60
190	37.72	5.24	2.14	-4.59	-3.51	5.09	38.16	6.17	0.69	0.68	0.85	0.60	0.85	0.59	0.69	0.68
200	38.59	5.28	4.01	-4.54	-4.33	5.04	38.84	5.46	0.53	0.48	0.74	0.48	0.74	0.48	0.53	0.48
210	38.82	5.21	2.53	-4.37	-3.27	5.05	39.01	5.70	0.62	0.56	0.36	0.47	0.36	0.47	0.62	0.55
220	38.59	5.84	3.09	-3.48	-3.82	4.53	38.78	6.28	0.47	0.22	0.57	0.30	0.57	0.31	0.47	0.24
230	39.01	6.54	3.06	-2.80	-3.67	4.29	39.06	6.88	0.81	0.77	0.53	0.47	0.53	0.47	0.81	0.77
250	38.23	23.07	8.50	-7.80	-8.55	10.15	37.96	23.82	28.71	48.52	15.15	15.03	7.40	13.08	32.70	51.14
260	36.85	6.06	6.27	-6.36	-5.57	9.07	36.42	6.11	34.47	27.82	12.55	15.46	12.55	15.46	34.47	27.83
270	29.40	4.45	2.43	-1.73	-0.41	3.64	27.21	5.94	46.01	49.64	13.89	22.14	13.89	22.14	46.01	49.64
280	51.11	-0.28	7.54	-4.83	-7.02	6.29	50.85	2.59	13.81	12.47	12.38	14.05	12.38	14.05	13.81	12.47
290	41.20	5.02	1.61	-2.95	-1.52	5.21	41.07	7.55	15.14	12.80	9.10	8.38	9.10	8.38	15.14	12.80
310	31.96	3.76	19.23	1.55	-17.80	3.20	32.56	6.92	23.15	19.16	18.35	18.10	18.35	18.10	23.15	19.16
320	40.82	1.26	-0.56	-2.55	1.29	7.76	42.02	4.87	13.93	8.95	6.88	6.60	6.88	6.60	13.93	8.95

Table 16 Zero Preswirl, PR = 20%, 15,200 rpm for $q = 0.386$

f	RZ _{xx}	Iz _{xx}	RZ _{xy}	Iz _{xy}	RZ _{yx}	Iz _{yx}	RZ _{yy}	Iz _{yy}	RZ _{xx}	Iz _{xx}	RZ _{xy}	Iz _{xy}	RZ _{yx}	Iz _{yx}	RZ _{yy}	Iz _{yy}
20	35.85	1.38	31.61	-17.74	-31.44	17.77	35.93	1.32	2.39	4.69	6.04	6.71	6.04	6.71	2.39	4.69
30	30.88	3.06	22.95	-12.34	-22.73	12.30	30.97	3.15	1.63	2.02	3.13	3.26	3.13	3.26	1.63	2.02
40	31.88	3.76	20.73	-13.31	-20.52	13.44	32.15	3.97	2.08	2.17	2.44	3.44	2.46	3.45	2.05	2.15
50	34.36	-14.12	10.76	-22.03	-10.74	22.21	34.17	-14.88	29.84	34.14	12.82	19.01	12.82	19.01	29.84	34.14
70	32.38	2.66	12.81	-13.64	-12.55	13.66	32.26	2.66	1.22	2.23	3.25	2.55	3.25	2.55	1.22	2.23
80	34.64	4.32	10.44	-12.43	-10.15	12.35	34.50	4.40	1.72	1.86	2.66	2.00	2.66	2.00	1.73	1.86
90	33.45	4.21	9.74	-12.88	-9.43	12.77	33.34	4.37	0.94	1.58	1.16	0.87	1.16	0.87	0.94	1.58
100	35.34	3.99	9.38	-12.49	-9.07	12.34	35.33	4.14	3.90	3.43	2.28	1.93	2.28	1.93	3.90	3.43
110	34.31	4.67	8.67	-11.00	-8.34	10.71	34.33	4.91	3.54	4.34	2.05	1.16	2.05	1.16	3.54	4.34
130	35.99	4.21	6.58	-10.73	-6.33	10.26	36.07	4.45	1.76	1.61	1.62	1.49	1.62	1.49	1.76	1.62
140	36.36	6.43	5.85	-9.76	-5.95	9.10	36.41	6.78	1.89	1.36	0.80	0.67	0.80	0.67	1.89	1.36
150	37.48	5.90	5.80	-10.19	-6.05	9.55	37.67	6.14	2.51	2.08	0.78	0.72	0.78	0.72	2.51	2.08
160	36.92	6.60	4.92	-9.10	-5.56	8.52	37.09	6.97	0.72	0.42	0.57	0.60	0.57	0.60	0.71	0.42
190	38.39	6.61	2.66	-7.34	-4.03	7.84	38.84	7.54	0.60	0.67	0.87	0.60	0.87	0.60	0.60	0.67
200	38.87	6.21	4.40	-6.75	-4.72	7.26	39.12	6.39	0.44	0.73	0.34	0.55	0.34	0.55	0.44	0.73
210	37.56	6.57	3.72	-5.96	-4.46	6.65	37.74	7.06	0.65	0.67	0.44	0.54	0.44	0.54	0.65	0.67
220	38.68	6.60	3.32	-5.50	-4.04	6.56	38.87	7.04	0.52	0.39	0.33	0.27	0.33	0.28	0.52	0.40
230	38.75	6.40	4.06	-4.74	-4.66	6.22	38.81	6.74	1.06	0.89	0.43	0.47	0.44	0.46	1.06	0.90
250	53.39	-3.56	-21.36	-30.29	21.30	32.63	53.12	-2.81	14.18	11.99	16.04	12.96	9.10	10.65	21.11	20.13
260	-24.18	-62.18	-33.06	43.14	33.76	-40.43	-24.61	-62.13	95.50	79.70	53.44	89.32	53.44	89.32	95.51	79.70
270	37.63	-20.71	-1.42	-1.28	3.44	3.19	35.45	-19.22	25.75	18.93	16.54	26.93	16.54	26.93	25.75	18.93
280	42.14	8.23	3.17	-6.12	-2.64	7.57	41.88	11.10	12.04	5.88	7.74	9.13	7.74	9.13	12.04	5.88
290	51.78	8.33	-14.07	0.80	14.16	1.46	51.65	10.86	8.59	19.24	22.79	37.59	22.79	37.59	8.59	19.24
310	53.65	1.81	4.99	-1.85	-3.56	6.61	54.25	4.97	10.96	8.35	13.23	9.12	13.23	9.12	10.96	8.35
320	54.75	6.94	-15.14	1.82	15.87	3.39	55.95	10.56	29.95	15.32	36.22	30.19	36.22	30.19	29.95	15.32

Table 17 Zero Preswirl, PR = 20%, 20,200 rpm for $q = 0.386$

f	RZ _{xx}	Iz _{xx}	RZ _{xy}	Iz _{xy}	RZ _{yx}	Iz _{yx}	RZ _{yy}	Iz _{yy}	RZ _{xx}	Iz _{xx}	RZ _{xy}	Iz _{xy}	RZ _{yx}	Iz _{yx}	RZ _{yy}	Iz _{yy}
20	35.85	1.38	31.61	-17.74	-31.44	17.77	35.93	1.32	2.39	4.69	6.04	6.71	6.04	6.71	2.39	4.69
30	30.88	3.06	22.95	-12.34	-22.73	12.30	30.97	3.15	1.63	2.02	3.13	3.26	3.13	3.26	1.63	2.02
40	31.88	3.76	20.73	-13.31	-20.52	13.44	32.15	3.97	2.08	2.17	2.44	3.44	2.46	3.45	2.05	2.15
50	34.36	-14.12	10.76	-22.03	-10.74	22.21	34.17	-14.88	29.84	34.14	12.82	19.01	12.82	19.01	29.84	34.14
70	32.38	2.66	12.81	-13.64	-12.55	13.66	32.26	2.66	1.22	2.23	3.25	2.55	3.25	2.55	1.22	2.23
80	34.64	4.32	10.44	-12.43	-10.15	12.35	34.50	4.40	1.72	1.86	2.66	2.00	2.66	2.00	1.73	1.86
90	33.45	4.21	9.74	-12.88	-9.43	12.77	33.34	4.37	0.94	1.58	1.16	0.87	1.16	0.87	0.94	1.58
100	35.34	3.99	9.38	-12.49	-9.07	12.34	35.33	4.14	3.90	3.43	2.28	1.93	2.28	1.93	3.90	3.43
110	34.31	4.67	8.67	-11.00	-8.34	10.71	34.33	4.91	3.54	4.34	2.05	1.16	2.05	1.16	3.54	4.34
130	35.99	4.21	6.58	-10.73	-6.33	10.26	36.07	4.45	1.76	1.61	1.62	1.49	1.62	1.49	1.76	1.62
140	36.36	6.43	5.85	-9.76	-5.95	9.10	36.41	6.78	1.89	1.36	0.80	0.67	0.80	0.67	1.89	1.36
150	37.48	5.90	5.80	-10.19	-6.05	9.55	37.67	6.14	2.51	2.08	0.78	0.72	0.78	0.72	2.51	2.08
160	36.92	6.60	4.92	-9.10	-5.56	8.52	37.09	6.97	0.72	0.42	0.57	0.60	0.57	0.60	0.71	0.42
190	38.39	6.61	2.66	-7.34	-4.03	7.84	38.84	7.54	0.60	0.67	0.87	0.60	0.87	0.60	0.60	0.67
200	38.87	6.21	4.40	-6.75	-4.72	7.26	39.12	6.39	0.44	0.73	0.34	0.55	0.34	0.55	0.44	0.73
210	37.56	6.57	3.72	-5.96	-4.46	6.65	37.74	7.06	0.65	0.67	0.44	0.54	0.44	0.54	0.65	0.67
220	38.68	6.60	3.32	-5.50	-4.04	6.56	38.87	7.04	0.52	0.39	0.33	0.27	0.33	0.28	0.52	0.40
230	38.75	6.40	4.06	-4.74	-4.66	6.22	38.81	6.74	1.06	0.89	0.43	0.47	0.44	0.46	1.06	0.90
250	53.39	-3.56	-21.36	-30.29	21.30	32.63	53.12	-2.81	14.18	11.99	16.04	12.96	9.10	10.65	21.11	20.13
260	-24.18	-62.18	-33.06	43.14	33.76	-40.43	-24.61	-62.13	95.50	79.70	53.44	89.32	53.44	89.32	95.51	79.70
270	37.63	-20.71	-1.42	-1.28	3.44	3.19	35.45	-19.22	25.75	18.93	16.54	26.93	16.54	26.93	25.75	18.93
280	42.14	8.23	3.17	-6.12	-2.64	7.57	41.88	11.10	12.04	5.88	7.74	9.13	7.74	9.13	12.04	5.88
290	51.78	8.33	-14.07	0.80	14.16	1.46	51.65	10.86	8.59	19.24	22.79	37.59	22.79	37.59	8.59	19.24
310	53.65	1.81	4.99	-1.85	-3.56	6.61	54.25	4.97	10.96	8.35	13.23	9.12	13.23	9.12	10.96	8.35
320	54.75	6.94	-15.14	1.82	15.87	3.39	55.95	10.56	29.95	15.32	36.22	30.19	36.22	30.19	29.95	15.32

Table 18 Zero Preswirl, PR = 30%, 10,200 rpm for $q = 0.386$

f	RZ _{xx}	Iz _{xx}	RZ _{xy}	Iz _{xy}	RZ _{yx}	Iz _{yx}	RZ _{yy}	Iz _{yy}	RZ _{xx}	Iz _{xx}	RZ _{xy}	Iz _{xy}	RZ _{yx}	Iz _{yx}	RZ _{yy}	Iz _{yy}
20	36.58	0.96	18.47	-6.79	-18.29	6.82	36.67	0.90	5.96	3.97	5.70	3.06	5.70	3.06	5.96	3.97
30	35.59	0.78	11.49	-15.39	-11.26	15.35	35.68	0.86	2.35	3.35	12.28	9.57	12.28	9.57	2.35	3.35
40	34.33	-0.50	12.33	-9.77	-12.13	9.91	34.60	-0.29	2.74	3.83	2.66	1.79	2.67	1.81	2.72	3.82
50	33.49	2.66	14.53	-7.40	-14.51	7.59	33.30	1.91	6.12	7.94	2.40	3.50	2.40	3.50	6.12	7.94
70	34.48	1.86	9.62	-9.55	-9.36	9.57	34.36	1.85	1.73	2.09	1.45	1.64	1.45	1.64	1.73	2.09
80	34.07	2.67	9.31	-6.71	-9.02	6.63	33.93	2.75	1.91	1.62	1.75	2.31	1.75	2.31	1.91	1.62
90	34.42	4.69	7.11	-8.60	-6.80	8.49	34.32	4.86	1.72	1.14	0.89	1.75	0.89	1.75	1.72	1.14
100	35.19	3.67	5.77	-7.83	-5.46	7.68	35.17	3.83	1.59	1.64	1.81	1.32	1.81	1.32	1.59	1.64
110	35.43	4.09	5.95	-7.75	-5.62	7.47	35.46	4.32	1.44	1.91	1.04	1.43	1.04	1.43	1.44	1.91
130	36.45	5.56	5.75	-7.49	-5.50	7.02	36.53	5.80	1.19	0.85	1.60	1.14	1.60	1.14	1.19	0.85
140	37.04	5.38	4.67	-7.38	-4.76	6.71	37.10	5.73	1.21	1.12	1.27	0.84	1.27	0.84	1.21	1.12
150	37.77	6.00	4.48	-6.99	-4.74	6.35	37.96	6.23	0.82	1.63	0.93	1.04	0.93	1.04	0.82	1.63
160	37.79	6.21	3.77	-7.02	-4.42	6.44	37.96	6.58	0.27	0.57	0.48	0.56	0.48	0.56	0.27	0.57
190	38.62	6.38	2.19	-4.79	-3.56	5.29	39.06	7.31	0.49	0.37	0.62	0.66	0.62	0.66	0.49	0.37
200	39.61	6.24	3.31	-4.98	-3.63	5.49	39.86	6.42	0.23	0.46	0.53	0.38	0.53	0.38	0.22	0.46
210	39.73	6.13	2.32	-4.51	-3.06	5.20	39.91	6.62	0.39	0.29	0.30	0.44	0.30	0.44	0.39	0.29
220	39.95	6.49	2.64	-3.84	-3.36	4.90	40.14	6.92	0.32	0.40	0.32	0.18	0.33	0.20	0.32	0.41
230	40.44	6.91	2.83	-3.04	-3.44	4.52	40.50	7.26	0.64	0.33	0.42	0.33	0.43	0.33	0.64	0.34
250	36.93	-28.61	7.53	-12.83	-7.58	15.18	36.66	-27.86	43.67	26.51	21.37	14.42	16.80	12.38	46.39	31.06
260	57.43	-19.34	16.40	-12.70	-15.70	15.41	57.01	-19.29	41.64	50.51	27.68	38.58	27.67	38.58	41.64	50.51
270	38.82	-2.02	8.55	2.27	-6.52	-0.36	36.64	-0.53	22.40	22.12	21.37	19.93	21.37	19.93	22.40	22.12
280	44.64	3.30	2.58	-4.35	-2.06	5.81	44.38	6.18	11.45	11.61	9.74	6.72	9.74	6.72	11.45	11.61
290	38.18	6.46	-1.28	0.01	1.37	2.24	38.05	8.99	12.42	9.98	13.39	13.17	13.39	13.17	12.42	9.98
310	35.16	6.57	15.87	-1.02	-14.44	5.78	35.76	9.73	20.20	18.66	13.13	8.08	13.13	8.07	20.20	18.66
320	36.65	9.45	4.19	-2.44	-3.46	7.65	37.85	13.07	13.36	14.97	10.26	14.14	10.26	14.14	13.36	14.97

Table 19 Zero Preswirl, PR = 30%, 15,200 rpm for $q = 0.386$

f	RZ _{xx}	Iz _{xx}	RZ _{xy}	Iz _{xy}	RZ _{yx}	Iz _{yx}	RZ _{yy}	Iz _{yy}	RZ _{xx}	Iz _{xx}	RZ _{xy}	Iz _{xy}	RZ _{yx}	Iz _{yx}	RZ _{yy}	Iz _{yy}
20	32.18	2.58	23.40	-5.78	-23.22	5.81	32.26	2.53	3.97	5.72	2.74	4.10	2.74	4.10	3.97	5.72
30	30.80	-0.48	21.46	-8.04	-21.24	8.00	30.89	-0.40	2.68	2.37	7.24	10.94	7.24	10.94	2.68	2.37
40	33.12	-0.32	18.04	-9.72	-17.84	9.86	33.39	-0.10	2.76	2.47	2.82	3.06	2.83	3.07	2.74	2.45
50	31.91	9.42	18.82	-9.13	-18.79	9.32	31.72	8.66	6.39	9.42	4.84	4.07	4.84	4.07	6.39	9.42
70	32.63	3.60	12.63	-10.64	-12.37	10.66	32.51	3.60	2.21	1.86	2.28	1.56	2.28	1.56	2.21	1.86
80	33.68	3.24	10.67	-11.84	-10.37	11.76	33.54	3.32	1.16	1.18	2.73	2.05	2.73	2.05	1.16	1.19
90	33.69	5.05	10.59	-10.85	-10.27	10.74	33.59	5.21	1.49	1.59	0.78	1.87	0.79	1.87	1.49	1.59
100	34.74	5.22	9.35	-10.04	-9.04	9.89	34.72	5.38	2.05	2.89	0.99	1.39	0.99	1.39	2.05	2.89
110	35.32	4.49	7.88	-10.51	-7.55	10.22	35.34	4.73	1.80	2.77	1.40	1.73	1.40	1.74	1.80	2.77
130	34.60	6.40	7.19	-8.72	-6.94	8.25	34.68	6.64	1.83	1.67	0.97	1.12	0.97	1.12	1.83	1.67
140	36.03	5.90	5.26	-8.60	-5.36	7.93	36.09	6.25	1.37	0.97	0.64	1.08	0.64	1.08	1.37	0.97
150	37.99	7.25	6.14	-8.92	-6.39	8.28	38.18	7.48	1.46	1.18	1.23	0.90	1.23	0.90	1.46	1.18
160	36.97	6.76	5.16	-8.33	-5.80	7.75	37.14	7.12	0.41	0.40	0.31	0.38	0.30	0.38	0.40	0.40
190	37.93	7.06	3.58	-6.36	-4.95	6.86	38.37	7.99	0.54	0.31	0.49	0.45	0.49	0.45	0.54	0.31
200	39.01	6.92	4.81	-6.64	-5.13	7.15	39.26	7.09	0.40	0.51	0.42	0.42	0.42	0.42	0.40	0.51
210	39.09	6.57	3.52	-5.68	-4.26	6.36	39.27	7.06	0.42	0.46	0.33	0.22	0.33	0.22	0.42	0.45
220	39.57	6.94	3.84	-5.41	-4.57	6.46	39.75	7.38	0.34	0.28	0.31	0.33	0.32	0.33	0.35	0.30
230	40.20	7.02	3.82	-4.50	-4.42	5.99	40.25	7.37	0.70	0.62	0.38	0.43	0.39	0.42	0.70	0.63
250	33.04	7.77	-1.67	-9.33	1.61	11.68	32.77	8.52	4.91	4.50	13.85	9.87	4.14	6.53	16.40	16.79
260	32.80	11.46	1.62	-7.88	-0.91	10.59	32.38	11.50	13.69	11.23	8.03	9.92	8.03	9.91	13.70	11.24
270	40.32	5.41	0.79	-6.86	1.23	8.77	38.14	6.90	19.29	24.09	13.20	10.83	13.20	10.83	19.30	24.09
280	41.45	6.25	0.43	-5.00	0.10	6.46	41.20	9.12	5.21	8.62	9.59	10.12	9.59	10.12	5.21	8.62
290	44.41	6.85	-2.95	2.63	3.04	-0.37	44.27	9.38	10.92	10.61	18.67	20.67	18.67	20.67	10.92	10.61
310	40.31	8.49	6.48	3.20	-5.05	1.56	40.90	11.65	12.89	16.43	4.83	10.10	4.83	10.10	12.89	16.43
320	38.55	4.25	5.17	-4.77	-4.43	9.98	39.75	7.86	14.14	14.49	10.81	16.53	10.81	16.53	14.14	14.49

Table 20 Zero Preswirl, PR = 30%, 20,200 rpm for $q = 0.386$

f	RZ _{xx}	Iz _{xx}	RZ _{xy}	Iz _{xy}	RZ _{yx}	Iz _{yx}	RZ _{yy}	Iz _{yy}	RZ _{xx}	Iz _{xx}	RZ _{xy}	Iz _{xy}	RZ _{yx}	Iz _{yx}	RZ _{yy}	Iz _{yy}
20	32.18	2.58	23.40	-5.78	-23.22	5.81	32.26	2.53	3.05	3.71	3.14	2.54	3.14	2.54	3.05	3.71
30	30.80	-0.48	21.46	-8.04	-21.24	8.00	30.89	-0.40	1.50	1.45	1.82	3.40	1.82	3.40	1.50	1.45
40	33.12	-0.32	18.04	-9.72	-17.84	9.86	33.39	-0.10	1.55	1.82	1.97	2.54	1.99	2.55	1.52	1.79
50	31.91	9.42	18.82	-9.13	-18.79	9.32	31.72	8.66	18.23	34.01	13.78	15.16	13.78	15.16	18.23	34.01
70	32.63	3.60	12.63	-10.64	-12.37	10.66	32.51	3.60	1.60	1.61	2.11	3.21	2.11	3.21	1.60	1.61
80	33.68	3.24	10.67	-11.84	-10.37	11.76	33.54	3.32	1.07	0.67	1.61	1.35	1.61	1.35	1.07	0.67
90	33.69	5.05	10.59	-10.85	-10.27	10.74	33.59	5.21	1.31	1.35	1.64	1.23	1.64	1.23	1.31	1.35
100	34.74	5.22	9.35	-10.04	-9.04	9.89	34.72	5.38	2.15	2.77	1.35	1.32	1.35	1.32	2.15	2.77
110	35.32	4.49	7.88	-10.51	-7.55	10.22	35.34	4.73	2.92	5.42	1.73	1.76	1.73	1.76	2.92	5.42
130	34.60	6.40	7.19	-8.72	-6.94	8.25	34.68	6.64	1.29	1.22	1.21	1.04	1.21	1.04	1.29	1.22
140	36.03	5.90	5.26	-8.60	-5.36	7.93	36.09	6.25	0.88	1.51	1.00	0.87	1.01	0.87	0.88	1.51
150	37.99	7.25	6.14	-8.92	-6.39	8.28	38.18	7.48	2.68	2.56	0.86	1.38	0.86	1.38	2.68	2.56
160	36.97	6.76	5.16	-8.33	-5.80	7.75	37.14	7.12	0.49	0.51	0.66	0.30	0.65	0.30	0.49	0.51
190	37.93	7.06	3.58	-6.36	-4.95	6.86	38.37	7.99	0.96	0.63	0.73	0.60	0.73	0.60	0.96	0.63
200	39.01	6.92	4.81	-6.64	-5.13	7.15	39.26	7.09	0.35	0.42	0.56	0.38	0.56	0.38	0.35	0.42
210	39.09	6.57	3.52	-5.68	-4.26	6.36	39.27	7.06	0.44	0.69	0.53	0.48	0.54	0.48	0.44	0.69
220	39.57	6.94	3.84	-5.41	-4.57	6.46	39.75	7.38	0.39	0.52	0.43	0.29	0.43	0.29	0.39	0.53
230	40.20	7.02	3.82	-4.50	-4.42	5.99	40.25	7.37	1.12	0.70	0.41	0.29	0.41	0.28	1.12	0.70
250	33.04	7.77	-1.67	-9.33	1.61	11.68	32.77	8.52	11.53	10.97	28.27	19.89	25.00	18.46	19.43	19.54
260	32.80	11.46	1.62	-7.88	-0.91	10.59	32.38	11.50	26.57	26.38	35.05	23.31	35.05	23.30	26.58	26.39
270	40.32	5.41	0.79	-6.86	1.23	8.77	38.14	6.90	26.06	13.79	19.94	20.14	19.94	20.14	26.06	13.79
280	41.45	6.25	0.43	-5.00	0.10	6.46	41.20	9.12	5.74	7.23	7.09	9.46	7.09	9.46	5.74	7.23
290	44.41	6.85	-2.95	2.63	3.04	-0.37	44.27	9.38	8.22	14.65	19.24	10.13	19.24	10.13	8.22	14.65
310	40.31	8.49	6.48	3.20	-5.05	1.56	40.90	11.65	7.65	8.96	6.57	11.26	6.57	11.26	7.65	8.96
320	38.55	4.25	5.17	-4.77	-4.43	9.98	39.75	7.86	18.88	11.91	10.20	16.55	10.20	16.55	18.88	11.91

Table 21 Zero Preswirl, PR = 40%, 10,200 rpm for $q = 0.386$

f	RZ _{xx}	Iz _{xx}	RZ _{xy}	Iz _{xy}	RZ _{yx}	Iz _{yx}	RZ _{yy}	Iz _{yy}	RZ _{xx}	Iz _{xx}	RZ _{xy}	Iz _{xy}	RZ _{yx}	Iz _{yx}	RZ _{yy}	Iz _{yy}
20	35.69	-1.33	21.85	-9.12	-21.67	9.15	35.77	-1.39	5.39	4.53	4.54	4.92	4.54	4.92	5.39	4.53
30	31.84	1.23	15.37	-10.69	-15.15	10.65	31.94	1.31	2.38	3.30	3.58	4.94	3.58	4.94	2.38	3.30
40	34.63	2.86	13.86	-10.33	-13.66	10.47	34.90	3.07	1.19	2.00	1.66	2.33	1.68	2.34	1.14	1.98
50	33.52	-0.94	11.08	-11.53	-11.06	11.72	33.33	-1.70	4.26	4.97	3.52	2.53	3.52	2.53	4.26	4.96
70	33.75	4.24	11.00	-8.26	-10.74	8.29	33.63	4.24	2.52	1.77	2.50	1.68	2.50	1.68	2.52	1.77
80	34.24	5.26	8.75	-8.34	-8.45	8.26	34.10	5.34	1.34	1.10	1.27	1.72	1.27	1.72	1.34	1.10
90	34.62	6.10	7.57	-9.25	-7.26	9.14	34.51	6.26	1.08	1.64	1.64	1.51	1.64	1.51	1.08	1.64
100	34.78	5.52	6.10	-8.52	-5.79	8.37	34.76	5.67	1.48	1.97	1.43	1.63	1.43	1.63	1.48	1.97
110	33.80	7.03	6.69	-8.24	-6.36	7.95	33.83	7.27	0.95	1.73	1.08	0.97	1.08	0.97	0.95	1.73
130	36.07	7.49	5.28	-7.18	-5.03	6.71	36.15	7.73	0.74	0.94	1.18	1.24	1.18	1.24	0.74	0.94
140	36.66	7.08	4.49	-7.04	-4.59	6.38	36.71	7.42	1.25	1.20	0.51	1.17	0.51	1.17	1.25	1.20
150	36.75	7.63	4.26	-7.20	-4.51	6.56	36.94	7.87	1.54	1.28	0.74	0.65	0.74	0.65	1.54	1.28
160	37.88	8.10	3.50	-7.06	-4.15	6.48	38.05	8.47	0.59	0.41	0.68	0.66	0.68	0.66	0.59	0.41
190	38.67	8.31	2.10	-4.81	-3.47	5.31	39.11	9.24	0.49	0.55	0.49	0.48	0.49	0.48	0.49	0.55
200	40.40	8.13	3.27	-5.15	-3.59	5.66	40.65	8.31	0.39	0.50	0.44	0.38	0.44	0.39	0.39	0.50
210	40.03	8.11	2.25	-4.11	-2.99	4.80	40.21	8.60	0.38	0.56	0.31	0.34	0.31	0.34	0.38	0.56
220	40.79	8.07	2.48	-3.91	-3.20	4.96	40.98	8.50	0.42	0.48	0.27	0.18	0.27	0.19	0.42	0.49
230	41.24	8.18	2.67	-3.06	-3.27	4.54	41.29	8.52	0.68	0.65	0.27	0.37	0.28	0.37	0.68	0.65
250	54.07	8.23	4.96	-2.10	-5.02	4.45	53.80	8.45	41.86	26.62	20.33	19.31	15.45	17.84	44.69	31.15
260	46.41	20.08	3.78	2.86	-3.07	-0.15	45.98	20.12	37.81	30.01	25.73	26.04	25.73	26.04	37.82	30.01
270	53.60	9.36	12.28	9.69	-10.26	-7.78	51.42	10.85	22.87	26.88	14.48	19.28	14.48	19.28	22.87	26.88
280	47.57	7.59	-4.95	-4.11	5.47	5.57	47.31	10.47	7.94	8.31	10.73	9.40	10.73	9.40	7.94	8.31
290	47.00	13.18	7.16	-4.95	-7.06	7.21	46.87	15.71	7.91	17.33	29.65	25.89	29.65	25.89	7.91	17.33
310	41.80	10.61	15.57	-3.29	-14.14	8.05	42.39	13.78	21.35	13.30	12.45	3.94	12.45	3.94	21.35	13.30
320	55.89	-6.05	-0.87	21.31	1.60	-16.10	57.09	-2.43	11.20	42.92	47.69	39.22	47.69	39.22	11.20	42.92

Table 22 Zero Preswirl, PR = 40%, 15,200 rpm for $q = 0.386$

f	RZ _{xx}	Iz _{xx}	RZ _{xy}	Iz _{xy}	RZ _{yx}	Iz _{yx}	RZ _{yy}	Iz _{yy}	RZ _{xx}	Iz _{xx}	RZ _{xy}	Iz _{xy}	RZ _{yx}	Iz _{yx}	RZ _{yy}	Iz _{yy}
20	34.34	-1.80	26.64	-11.76	-26.47	11.79	34.42	-1.86	2.68	3.43	3.21	3.70	3.21	3.70	2.68	3.43
30	29.14	2.74	17.66	-11.20	-17.44	11.17	29.23	2.83	2.52	1.62	2.68	3.07	2.68	3.07	2.52	1.62
40	30.75	5.48	20.78	-12.93	-20.58	13.06	31.02	5.69	2.42	3.39	5.41	2.84	5.41	2.85	2.39	3.38
50	29.74	9.17	15.55	-10.65	-15.53	10.84	29.56	8.41	14.75	14.55	7.86	7.75	7.86	7.75	14.75	14.55
70	34.07	5.58	12.39	-14.03	-12.13	14.05	33.95	5.58	1.52	1.28	2.34	1.77	2.34	1.77	1.52	1.28
80	33.33	5.52	11.27	-12.42	-10.98	12.34	33.19	5.59	1.62	1.80	1.12	1.59	1.12	1.59	1.62	1.80
90	33.92	5.93	8.57	-11.85	-8.26	11.74	33.81	6.09	2.01	1.40	1.71	1.69	1.71	1.69	2.01	1.40
100	35.11	6.16	8.54	-11.12	-8.22	10.97	35.09	6.31	2.57	2.61	1.37	1.58	1.37	1.58	2.57	2.61
110	35.80	8.74	8.78	-11.18	-8.45	10.89	35.83	8.97	3.74	3.22	1.85	1.82	1.85	1.82	3.74	3.22
130	35.93	7.86	6.89	-9.98	-6.64	9.51	36.01	8.10	1.43	1.89	1.72	1.61	1.72	1.61	1.43	1.90
140	37.11	7.43	5.61	-9.18	-5.71	8.52	37.16	7.78	1.95	0.93	1.07	0.97	1.07	0.97	1.95	0.93
150	37.61	9.62	6.63	-10.08	-6.88	9.44	37.80	9.86	2.10	2.76	1.16	1.32	1.16	1.32	2.10	2.76
160	37.98	8.08	3.93	-8.96	-4.58	8.38	38.14	8.45	0.54	0.63	0.73	0.63	0.73	0.63	0.54	0.63
190	39.13	8.42	2.69	-6.98	-4.07	7.48	39.57	9.35	1.22	0.60	0.48	0.55	0.48	0.55	1.22	0.60
200	40.40	8.22	4.10	-6.83	-4.43	7.34	40.66	8.40	0.60	0.59	0.51	0.52	0.52	0.52	0.60	0.59
210	39.48	8.77	3.20	-5.75	-3.94	6.44	39.66	9.25	0.42	0.50	0.39	0.38	0.39	0.38	0.42	0.50
220	40.46	8.08	3.18	-4.75	-3.90	5.80	40.65	8.52	0.38	0.38	0.33	0.49	0.33	0.49	0.38	0.39
230	41.02	8.01	3.91	-4.33	-4.52	5.81	41.07	8.35	0.63	1.24	0.18	0.43	0.19	0.43	0.63	1.24
250	28.26	8.23	-14.95	-8.28	14.90	10.63	27.99	8.45	14.55	21.49	23.32	15.45	19.22	13.57	21.36	26.90
260	14.67	36.20	17.54	-1.30	-16.83	4.01	14.24	36.25	35.86	28.87	25.64	30.10	25.64	30.10	35.86	28.87
270	40.79	2.45	-8.15	-5.85	10.18	7.76	38.61	3.94	26.93	21.80	17.72	20.22	17.72	20.22	26.93	21.80
280	43.90	15.58	-3.00	-6.16	3.52	7.62	43.64	18.45	6.85	9.62	12.06	7.47	12.06	7.47	6.85	9.62
290	61.91	10.54	-11.02	-6.35	11.11	8.61	61.78	13.07	18.92	15.86	19.86	30.97	19.86	30.97	18.92	15.86
310	39.66	-2.49	11.84	-1.84	-10.41	6.60	40.26	0.68	14.51	10.82	8.45	11.95	8.45	11.94	14.51	10.82
320	39.73	4.75	6.19	-2.74	-5.46	7.95	40.93	8.37	25.54	15.29	21.45	28.31	21.45	28.31	25.54	15.29

Table 23 Zero Preswirl, PR = 40%, 20,200 rpm for $q = 0.386$

f	RZ _{xx}	Iz _{xx}	RZ _{xy}	Iz _{xy}	RZ _{yx}	Iz _{yx}	RZ _{yy}	Iz _{yy}	RZ _{xx}	Iz _{xx}	RZ _{xy}	Iz _{xy}	RZ _{yx}	Iz _{yx}	RZ _{yy}	Iz _{yy}
20	33.76	-2.06	32.30	-19.93	-32.12	19.96	33.85	-2.12	4.62	2.25	5.33	7.01	5.33	7.01	4.62	2.25
30	27.87	3.96	24.58	-9.53	-24.35	9.49	27.97	4.05	2.34	2.56	4.03	5.51	4.02	5.51	2.34	2.56
40	32.07	7.13	23.78	-13.86	-23.58	14.00	32.34	7.35	2.26	1.51	1.88	2.91	1.90	2.92	2.23	1.48
50	18.47	-0.79	9.47	-10.69	-9.45	10.88	18.28	-1.55	15.97	19.69	10.75	9.87	10.75	9.87	15.97	19.69
70	34.05	3.98	14.04	-15.18	-13.79	15.21	33.93	3.97	1.71	1.52	1.86	2.48	1.86	2.48	1.71	1.52
80	34.97	3.92	12.78	-15.69	-12.49	15.61	34.83	3.99	1.87	1.45	1.70	2.28	1.70	2.28	1.87	1.46
90	33.35	6.19	10.48	-13.84	-10.17	13.73	33.24	6.35	1.88	1.31	1.03	1.40	1.03	1.40	1.88	1.31
100	33.76	3.76	8.29	-12.92	-7.97	12.77	33.74	3.91	3.50	3.71	1.55	1.28	1.55	1.28	3.50	3.71
110	34.03	8.08	9.23	-11.91	-8.91	11.62	34.06	8.32	4.03	3.55	1.68	1.59	1.68	1.59	4.03	3.55
130	36.57	5.22	7.03	-11.67	-6.78	11.21	36.64	5.46	1.51	2.87	1.34	1.37	1.34	1.37	1.51	2.87
140	37.17	7.60	6.28	-10.84	-6.38	10.17	37.23	7.95	0.83	2.12	0.97	0.83	0.97	0.83	0.83	2.12
150	39.11	9.95	6.72	-11.40	-6.97	10.76	39.30	10.19	2.18	3.18	1.22	1.03	1.22	1.03	2.18	3.17
160	38.46	7.46	4.97	-10.98	-5.61	10.40	38.62	7.82	0.52	0.59	0.57	0.72	0.57	0.72	0.52	0.59
190	38.96	7.48	3.02	-7.30	-4.40	7.80	39.40	8.41	0.75	0.98	0.87	0.47	0.87	0.47	0.75	0.99
200	39.74	6.90	4.14	-7.26	-4.46	7.77	39.99	7.07	0.56	0.42	0.53	0.47	0.53	0.47	0.56	0.42
210	39.64	7.51	3.35	-6.31	-4.09	6.99	39.83	8.00	0.63	0.58	0.44	0.62	0.44	0.62	0.63	0.58
220	40.61	7.44	3.59	-5.66	-4.31	6.71	40.80	7.87	0.60	0.57	0.59	0.51	0.59	0.52	0.61	0.58
230	41.32	7.07	3.98	-5.56	-4.58	7.05	41.38	7.42	1.19	0.59	0.27	0.39	0.28	0.38	1.19	0.60
250	34.33	8.23	-7.34	2.57	7.29	-0.22	34.06	8.45	8.34	7.16	17.12	12.47	10.89	10.04	17.73	17.69
260	48.11	12.13	-3.34	-6.18	4.04	8.89	47.68	12.09	20.92	24.40	16.90	15.89	16.90	15.89	20.93	24.41
270	40.49	21.06	-3.71	2.81	5.74	-0.90	38.31	22.55	24.44	41.44	21.26	35.13	21.26	35.13	24.44	41.44
280	44.43	4.42	2.30	-4.43	-1.78	5.89	44.17	7.29	9.62	12.34	9.08	14.27	9.08	14.27	9.62	12.34
290	44.65	49.76	25.61	-8.01	-25.52	10.27	44.52	52.29	33.45	10.31	64.06	26.72	64.06	26.72	33.45	10.73
310	44.35	-1.56	1.29	-8.61	0.14	13.37	44.95	1.60	7.03	9.44	7.12	7.85	7.12	7.84	7.03	9.44
320	47.63	16.98	-6.41	-16.15	7.15	21.36	48.83	20.60	15.97	44.33	29.45	57.92	29.45	57.92	15.97	44.33

VITA

Name: Daniel Eduardo van der Velde Álvarez
Date of Birth: July 18, 1980 (Venezuela)
Education: B.S. Mechanical Engineering, Universidad Simón Bolívar, March 2004
M.S. Mechanical Engineering, Texas A&M University, December 2006

Email: dvander@tamu.edu
Address: 5510 S. Rice Ave. Apt# 1431
Houston, Texas 77081